Redox Biology 15 (2018) 532–547

Contents lists available at ScienceDirect

Redox Biology

journal homepage: www.elsevier.com/locate/redox

Research paper

A glutaredoxin in the mitochondrial intermembrane space has stage-specific functions in the thermo-tolerance and proliferation of African trypanosomes

Samantha Ebersoll[a], Blessing Musunda[a], Torsten Schmenger[a], Natalie Dirdjaja[a], Mariana Bonilla[b], Bruno Manta[b,1], Kathrin Ulrich[a,2], Marcelo A. Comini[b], R. Luise Krauth-Siegel[a,*]

[a] Biochemie-Zentrum der Universität Heidelberg, Im Neuenheimer Feld 328, 69120 Heidelberg, Germany
[b] Group Redox Biology of Trypanosomes, Institut Pasteur de Montevideo, Mataojo 2020, CP 11400, Montevideo, Uruguay

ARTICLE INFO

Keywords:
Glutaredoxin
Tryparedoxin
Trypanothione
Trypanosoma brucei
Mitochondrion

ABSTRACT

Trypanosoma brucei glutaredoxin 2 (Grx2) is a dithiol glutaredoxin that is specifically located in the mitochondrial intermembrane space. Bloodstream form parasites lacking Grx2 or both, Grx2 and the cytosolic Grx1, are viable *in vitro* and infectious to mice suggesting that neither oxidoreductase is needed for survival or infectivity to mammals. A 37 °C to 39 °C shift changes the cellular redox milieu of bloodstream cells to more oxidizing conditions and induces a significantly stronger growth arrest in wildtype parasites compared to the mutant cells. Grx2-deficient cells ectopically expressing the wildtype form of Grx2 with its C31QFC34 active site, but not the C34S mutant, regain the sensitivity of the parental strain, indicating that the physiological role of Grx2 requires both active site cysteines. In the procyclic insect stage of the parasite, Grx2 is essential. Both alleles can be replaced if procyclic cells ectopically express authentic or C34S, but not C31S/C34S Grx2, pointing to a redox role that relies on a monothiol mechanism. RNA-interference against Grx2 causes a virtually irreversible proliferation defect. The cells adopt an elongated morphology but do not show any significant alteration in the cell cycle. The growth retardation is attenuated by high glucose concentrations. Under these conditions, procyclic cells obtain ATP by substrate level phosphorylation suggesting that Grx2 might regulate a respiratory chain component.

1. Introduction

Glutaredoxins (Grxs) are ubiquitous small oxidoreductases that belong to the thioredoxin superfamily and play crucial roles in the redox homeostasis of the cell (for reviews see [1,21,65]). All organisms have an individual set of isoforms that occur in the cytosol, mitochondria and nucleus. Based on the primary structure, two main groups are distinguishable, monothiol Grxs containing one or more CXXS motif(s) and the more classical dithiol Grxs with a CXXC active site sequence (mostly CPYC) [36]. Dithiol Grxs were first identified as highly efficient electron donors for ribonucleotide reductase and thus for the synthesis of the DNA building blocks [36,66]. Like thioredoxins, dithiol Grxs participate in a wide variety of biological processes, many of them can catalyze the reduction of protein disulfides using both active site cysteine residues albeit usually at lower efficiency than thioredoxins [37]. Grxs have been shown to play distinct roles in the sensitivity of various cells towards oxidative stressors [1,10,21,39,41]. A remarkable recent finding is that limiting amounts of the cytosolic Grxs in the mitochondrial intermembrane space (IMS) of *Saccharomyces cerevisiae* provide a kinetic barrier that prevents the reduction of target proteins by glutathione (GSH) [31].

A unique feature of dithiol Grxs is their ability to catalyze redox reactions using only the first cysteine (monothiol reactions). Generally, the functions of Grxs are closely linked to the GSH system since (i) their reduced form is regenerated by thiol/disulfide exchange of the oxidized protein with GSH, where the GSSG formed is then reduced by

Abbreviations: AMS, 4-acetamido-4′-maleimidylstilbene-2,2′-disulfonic acid; ASCT, acetate:succinate-CoA-transferase; BS, bloodstream; cTXNPx, cytosolic 2-Cys-peroxiredoxin; GR, glutathione reductase; Grx, glutaredoxin; Gsp, glutathionylspermidine; HED, (hydroxyethyl)disulfide; KO, knockout; IMS, intermembrane space; LipDH, lipoamide dehydrogenase; 2-ME, 2-mercaptoethanol; MM(PEG)12, methyl-PEG12-maleimide; mTXNPx, mitochondrial 2-Cys-peroxiredoxin; PC, procyclic; RNAi, RNA interference; *S. cerevisiae*, *Saccharomyces cerevisiae*; SKO, single knockout; *T. brucei*, , *Trypanosoma brucei*; *T. cruzi*, *Trypanosoma cruzi*; TCEP, tris(2-carboxyethyl)phosphine; Tpx, tryparedoxin; tet, tetracycline; $T(SH)_2$, trypanothione; TS_2, trypanothione disulfide; WT, wildtype

* Correspondence to: Biochemie-Zentrum der Universität Heidelberg, Im Neuenheimer Feld 328, D-69120 Heidelberg, Germany.
E-mail address: luise.krauth-siegel@bzh.uni-heidelberg.de (R.L. Krauth-Siegel).
[1] Current address: Brigham and Women's Hospital and Harvard Medical School, 77 Avenue Louis Pasteur, NRB 435, Boston, Massachusetts, 02115, USA.
[2] Current address: Department of Molecular, Cellular, and Developmental Biology, University of Michigan, MI 48109, Ann Arbor, Michigan, USA.

https://doi.org/10.1016/j.redox.2018.01.011
Received 28 December 2017; Accepted 23 January 2018
Available online 31 January 2018

glutathione reductase, and (ii) they catalyze with high efficiency and selectivity the reversible S-glutathionylation of proteins. The latter mechanism may be employed to protect reactive cysteine residues in distinct proteins from irreversible over-oxidation as well as for redox signaling pathways that could mediate critical cellular functions like proliferation and apoptosis [1,21,41,65].

Trypanosomatids, such as *Trypanosoma brucei,* the causative agent of African sleeping sickness and Nagana cattle disease, lack glutathione reductases and thioredoxin reductases and their thiol metabolism is based on the low molecular mass dithiol trypanothione [bis(glutathionyl)spermidine, $T(SH)_2$] and trypanothione reductase (for reviews see [33,34,44]). $T(SH)_2$ is synthesized from two molecules of GSH that are covalently linked by spermidine with glutathionylspermidine (Gsp) as intermediate [11,51]. The $T(SH)_2$ system is involved in the synthesis of DNA precursors as well as the detoxification of hydroperoxides. The reactions are mediated by tryparedoxin (Tpx). This essential and parasite-specific oxidoreductase is a distant member of the thioredoxin-type protein family and fulfils many of the functions known to be catalyzed by thioredoxins and/or Grxs in other organisms [13,59]. Despite the absence of a classical glutathione system, trypanosomatids contain appreciable concentrations of free GSH as well as a repertoire of distinct Grxs [12,33]. Recently we showed that as response to exogenous and endogenous oxidative stresses, the mammalian bloodstream (BS) form of *T. brucei* can undergo protein S-glutathionylation and S-trypanothionylation [64].

The *T. brucei* genome encodes genes for three monothiol Grxs as well as two dithiol Grxs (Grx1 and Grx2) [12]. Grx1 represents a canonical dithiol Grx whereas Grx2 has sequence features exclusively found in trypanosomatid organisms [12]. In *T. brucei*, Grx1 is a cytosolic protein whereas Grx2 is located in the mitochondrion and preliminary studies suggest a localization in the intermembrane space (IMS) [9]. Interestingly, *Trypanosoma cruzi*, the causative agent of Chagas' disease, encodes a single *grx* gene. The protein has an overall sequence identity of 80% with *T. brucei* Grx2 and is located in the cytosol [46].

The catalytic properties of recombinant *T. brucei* Grx1 and Grx2 as well as *T. cruzi* Grx have been studied in some detail [9,46,47]. The reduced form of the proteins with the active site cysteines (Cys31 and Cys34 in *T. brucei* Grx2) in the thiol state is regenerated from the intramolecular disulfide by spontaneous thiol/disulfide exchange with $T(SH)_2$, reactions that are at least three orders of magnitude faster compared to those with GSH [9,46]. The trypanosomal Grxs accelerate the reduction of GSSG by $T(SH)_2$ which again reflects their close link with the trypanothione metabolism. Both *T. brucei* Grxs and *T. cruzi* Grx catalyze the reduction of the mixed disulfide between GSH and either 2-mercaptoethanol or cysteine residues of various model proteins, a reaction that is not taken over, at least to a physiological competent degree, by Tpx [9,43,46]. Indeed, the cytosolic Grx1 has been shown to contribute to about 50% of the deglutathionylation capacity of infective *T. brucei* [49] and facilitates the reversion of stress-induced protein S-thiolation [64]. Nonetheless, at variance with Tpx [13], parasites lacking Grx1 are fully proliferative *in vitro* and *in vivo*, and even display a marked thermoresistance when grown at 39 °C [49]. In contrast, RNA-interference (RNAi) against Grx2 causes growth retardation of procyclic (PC) insect stage cells [9] indicating life cycle specific functions of Grxs in trypanosomes. Supporting this assumption, overexpression of Grx in the amastigote intracellular form of *T. cruzi* confers resistance against oxidative damage and promotes parasite growth while in non-infective parasites it induces apoptosis [46].

Here we investigated the molecular and biological details of the overall contribution of the Grx-dependent metabolism for parasite survival in an animal host as well as of the indispensability of Grx2 for PC trypanosomes. We show that Grx2 specifically localizes to the IMS of the mitochondrion and that its biological functions require the presence of both (in BS cells) or only the first (in PC cells) of the active site cysteine residues. Grx2 was dispensable for infective trypanosomes but, as observed for Grx1 KO cells, its absence increased the thermo-tolerance of BS cells. Thus, from a therapeutic point of view, the parasite Grxs can be ruled out as putative drug target molecules. Remarkably, the temperature rise lowered the cellular $T(SH)_2/TS_2$ ratio and increased the level of S-glutathionylated proteins, whereby these effects were Grx-independent. In contrast, Grx2 is essential in PC cells. The insect stage requires a redox-active Grx2 for viability. RNAi-mediated downregulation of the oxidoreductase resulted in cells with elongated morphology that were irreversibly arrested in proliferation.

2. Material and methods

2.1. Material

Insulin, digitonin, diamide, tetracycline (tet), DAPI, (hydroxylethyl) disulfide (HED), 2-mercaptoethanol (2-ME) and sodium (meta) arsenite were purchased from Sigma-Aldrich. Puromycin dihydrochloride, hygromycin B, and blasticidin hydrochloride were from Roth, Karlsruhe. Fetal calf serum (FCS) was from Biochrome, H_2O_2, G418 and mono (bromo)bimane (mBBr) from Merck. 5,5′-Dithio-bis-(2-nitrobenzoic acid) (DTNB) was ordered from Serva, Heidelberg, and 4-acetamido-4′-maleimidylstilbene-2,2′-disulfonic acid (AMS) from Life Technologies. The Bond Breaker tris(2-carboxyethyl)phosphine (TCEP) solution and methyl-PEG12-maleimide [MM(PEG)12] were from Thermo Scientific. Recombinant Grx2 was produced as described [9]. Recombinant human glutathione reductase (GR) was a kind gift of Dr. Heiner Schirmer, Heidelberg University. Polyclonal guinea pig antisera against *T. brucei* Grx1 as well as rabbit antisera against *T. brucei* cytosolic 2-Cys-peroxiredoxin (cTXNPx), lipoamide dehydrogenase (LipDH) and Tpx were obtained previously [9,13,58]. Polyclonal guinea pig antibodies against the mitochondrial *T. brucei* 2-Cys-peroxiredoxin (mtTXNPx) as well as rabbit and guinea pig antibodies against Grx2 were generated by Eurogentec. Polyclonal rabbit antibodies against acetate: succinate-CoA-transferase (ASCT) were a kind gift from Dr. Frédéric Bringaud, University of Bordeaux. Goat anti guinea pig IgG were purchased from Santa Cruz Biotechnology. Goat anti rabbit IgG were from Thermo Scientific or Santa Cruz Biotechnology. The pHD vectors used for *T. brucei* transfection were kindly provided by Dr. Christine Clayton, Heidelberg University. All primers were synthesized by Eurofins MWG Operons, Ebersberg, Germany. The plasmids were sequenced by Euro-Fins MWG Operons or GATC Biotech AG, Konstanz, Germany.

2.2. Cultivation of T. brucei under various conditions

The parasites used in this work were of the *T. brucei brucei* 449 cell line which is a descendant of the Lister 427 strain [17]. BS parasites were cultivated in HMI-9 medium at 37 °C in a humidified incubator with 5% CO_2. If not stated otherwise, PC cells were grown at 27 °C in MEM-Pros medium. Both media were supplemented with 10% (v/v) heat-inactivated FCS, 50 units/ml penicillin, and 50 μg/ml streptomycin. In addition, the HMI-9 medium and MEM-Pros medium contained 0.2 μg/ml and 0.5 μg/ml, respectively, of phleomycin to select for cells containing the tet repressor gene [62,6]. To study the temperature sensitivity of BS parasites, WT parasites and the Grx mutants were grown at 39 °C in the presence or absence of 1 μg/ml tet in medium without hygromycin. The response of BS cells towards hydrogen peroxide, diamide and sodium arsenite was studied in HMI-9 medium lacking cysteine and 2-ME. The response of PC cells towards hydrogen peroxide and diamide was followed in SDM-79 medium. A putative temperature phenotype of Grx2-depleted PC cells was studied at 37 °C. The proliferation of PC under high glucose conditions was followed in MEM-Pros medium supplemented with 10 mM glucose. Cells were counted in a Neubauer chamber.

2.3. Cloning of constructs for deletion and/or ectopic overexpression of grx2 species in T. brucei

Genomic DNA was isolated from BS *T. brucei* using the Qiagen DNeasy Blood and Tissue kit. For the deletion of both *grx2* alleles, the 5′ untranslated region (*utr*) of *grx2* (TriTryp code: Tb927.1.1770) was amplified by PCR with *Pfu* polymerase and Grx2-5′−1F and Grx2-5′−2R as primers, generating a fragment of 388 bp. All primers used in this work are listed in Table S1. The 3′ *utr* was amplified using the primers Grx2-3′−7F and Grx2-3′−4R, yielding a 416 bp fragment. Both fragments were purified from a 2% agarose gel using the Zymoclean Gel DNA Recovery kit. With the pHD1747-*grx1*-KO vector [49] as template, the 5′ and 3′ *utr* of *grx1* were stepwise released by digestion with *Xho*I/*Hin*dIII and *Eco*RI/*Not*I, respectively, and replaced by the *grx2 utr* fragments generating pHD1747-*grx2*-KO. The blasticidin resistance gene in the pHD1748-*grx1*-KO vector [49] was removed by digestion with *Hin*dIII and *Eco*RI and replaced with the neomycin resistance gene which was obtained from pHD2171 by digestion also with *Hin*dIII and *Eco*RI. Subsequently, the 5′ and 3′ *utr* of *grx1* were stepwise replaced by the *grx2 utr* fragments, generating pHD1748 (*neo*)-*grx2*-KO.

Since preliminary work had revealed largely cytosolic localization of a C-terminally myc-tagged version of Grx2, a vector was generated that allowed tet-inducible expression of a tag-free ectopic copy of Grx2 in the parasites. For this purpose, a stop codon was introduced after the coding sequence in the pHD1700/*grx2*-c-myc2 vector [9] by the QuickChange Multi Site-Directed Mutagenesis Kit and the primers Grx2-Stop-F/Grx2-Stop-R resulting in pHD1700/*grx2*. For the expression of C34S and C31S/C34S Grx2 mutants, the pHD1700/*grx2* vector was mutated using the primer pair Grx2-C34-F/Grx2C34S-R and Grx2-Dmut-F/Grx2-Dmut-R, respectively. The products were pHD1700/*grx2c34s* and pHD1700/*grx2c31s/c34s*.

2.4. Generation of BS Grx2 KO, conditional Grx2 KO and Grx1/Grx2 KO cell lines

To obtain Grx2 KO cells, 4×10^7 BS *T. brucei* were harvested in the logarithmic growth phase. 12 µg of pHD1747-*grx2*-KO and pHD1748(*neo*)-*grx2*-KO, respectively, was digested with *Xho*I and *Not*I, ethanol-precipitated, mixed with 100 µl human T cell nucleofactor solution and added to the cell pellet. Transfection was performed in the Amaxa nucleofactor electroporator with the program X-001. The parasites were grown overnight in 50 ml of HMI-9 medium without any selecting antibiotic. Afterwards the cells were seeded in 24-well plates by serial dilutions, selecting with 0.2 µg/ml puromycin or 2.5 µg/ml neomycin as outlined previously [49]. Verified single KO (SKO) cells were transfected with the respective other deletion cassette and clones selected with both antibiotics. Deletion of both *grx2* alleles was verified by PCR and Western blot analyses.

Conditional BS Grx2 KO cells were obtained by transfecting Grx2 KO cells with *Not*I-linearized pHD1700/*grx2*, pHD1700/*grx2-c34s* or pHD1700/*grx2-c31s/c34s*. Stably-transfected clones were selected with 10 µg/ml of hygromycin. BS cell lines that lack both Grxs (Grx1/Grx2 KO) were obtained by transfecting Grx1 KO cells [49] with pHD1747-*grx2*-KO and pHD1748(*neo*)-*grx2*-KO as outlined above.

2.5. Generation of PC conditional Grx2 KO cell lines

PC *T. brucei* were transfected with *Xho*I/*Not*I-digested pHD1747-*grx2*-KO or pHD1748 (*neo*)-*grx2*-KO as outlined above for BS cells and clones selected by 2 µg/ml puromycin and 30 µg/ml G418, respectively. Grx2 SKO cells were obtained. However, subsequent transfection with the respective second deletion cassette yielded one double-resistant cell line that still had a *grx2* gene. Therefore, Grx2 SKO (puro) cells were transfected with *Not*I-linearized pHD1700/*grx2,* pHD1700/*grx2-c34s* or pHD1700/*grx2-c31s/c34s* and cell lines selected with 2 µg/ml puromycin and 50 µg/ml hygromycin. The Grx2 SKO (puro) clones that harbored a tet-inducible ectopic copy of either *grx2*, *grx2-c34s* or *grx2-c31s/c34s* were grown overnight in MEM-Pros medium containing 2 µg/ml puromycin, 50 µg/ml hygromycin, and 100 ng/ml tet and then transfected with the *Xho*I/*Not*I-digested pHD1748(neo)-*grx2*-KO construct. After culturing the cells overnight at 27 °C in the presence of hygromycin and tet (but no puromycin or G418), cell lines were selected in medium containing all four antibiotics.

2.6. Western blot analyses

Western blot analyses as well as the removal of bound antibodies were conducted as described previously [9,49]. Proteins were separated by SDS-PAGE, blotted onto a PVDF membrane and reacted with antibodies against Grx1 (1:800), Grx2 (rabbit, 1:200 or guinea pig, 1:500), cTXNPx (1:3000), Tpx (1:2000), LipDH (1:1000), ASCT (1:500), and mtTXNPx (1:1000). The secondary goat antibodies were diluted 1:10,000 (guinea pig) and 1:20,000 (rabbit). Bands were visualized by chemiluminescence using the Super-Signal West Pico Kit (Pierce) or the Western BLoT Ultra Sensitive HRP Substrate (Takara).

2.7. Immunofluorescence microscopy

The immunofluorescence microscopy was done as described previously [26,49].

2.8. HPLC analysis of mBBr-labeled parasite thiols

The level of free thiols, free thiols and disulfides and protein-bound thiols was determined as described previously [64]. Shortly, about 1×10^8 BS T. *brucei* were grown at 37 °C or 39 °C, washed with PBS and an aliquot was removed for counting. Proteins were precipitated by tri (chloro)acetic acid (TCA) treatment. The supernatant was split into two parts. One sample was directly labeled with mBBr. The other one was treated with TCEP followed by mBBr derivatization. The protein pellet was dissolved and treated with TCEP. After precipitation of the proteins, the supernatant containing the released thiols was reacted with mBBr. The samples were subjected to HPLC analysis and fluorescence detection. The thiols were quantified by comparing integrated peak areas between the sample and standard curves of each thiol derivative. The cellular concentration was calculated by normalizing to the cell number and a cell volume of 58 fl [50].

2.9. Subcellular localization of Grx2

For BS cells, the differential membrane permeabilization was done essentially as described previously for PC cells [9]. For each digitonin concentration, 6.5×10^7 cells were used. Digitonin was added to the cell pellets resulting in increasing digitonin: protein ratios (mg/mg). The samples were incubated at 25 °C for 5 min and centrifuged. The supernatants were mixed with 4 × sample buffer containing 8 M urea and 0.2 mg/ml DNase. The pellets were washed with PBS and dissolved in 1 × sample buffer. All samples were subjected to Western blot analysis.

To distinguish between a putative localization of Grx2 in the matrix or IMS of the mitochondrion, per sample, 7×10^7 PC *T. brucei* were harvested, washed with PBS followed by 10 mM Tris-HCl, 150 mM NaCl, 1 mM EDTA, pH 7.4. All subsequent steps were carried out at 4 °C. The cells were re-suspended in 100 µl of the respective digitonin solution, incubated for 4 min and centrifuged. The supernatants were directly treated for 5 min with 10 mM TCEP followed by 15 min with 15 mM MM(PEG)12. The pellets were washed twice with 20 mM Tris, 0.6 M sorbitol, 0.5 M NaCl, pH 7.4, re-suspended in 100 µl buffer and treated with TCEP and MM(PEG)12. The control samples obtained the same volume of buffer. The reaction was stopped by adding 38 mM 2-ME. The samples were mixed with 4 × sample buffer containing 0.05 mg/ml DNase I and subjected to Western blot analysis.

2.10. In vivo experiments

The animal protocols used in this work were approved by the Animal Use and Ethic Committee (CEUA) of the Institut Pasteur Montevideo (Protocol 2009_1_3284) and are in accordance with FELASA guidelines and the National law for Laboratory Animal Experimentation. The infection experiments were carried out using 6–8 weeks old female Balb/cJ mice (six per group) hosted at the Transgenic and Experimental Animal Unit (Institut Pasteur de Montevideo) as described previously [26,49,58]. Animals from each group were infected intraperitoneally (i.p.) with 10^4 WT, Grx2 KO, Grx1/Grx2 KO cells as well as Grx2 KO cells ectopically expressing a Grx2 copy.

The parasites were harvested in the exponential growth phase and resuspended in 0.3 ml fresh medium. The health status and survival of the animals were monitored daily. The parasitemia levels were assessed from day 4 post-infection onwards. Briefly, blood taken from the submandibular sinus (5–25 µl) was collected in a tube containing 5 µl of tripotassium ethylenediamine tetracetic acid (K_3EDTA, DELTALAB) as anticoagulant. In some cases, 10 µl PBS-1% (w/v) glucose was added to the blood to maintain parasite viability during sample processing. After thorough homogenization, an aliquot was diluted 1:20 in red cell lysis buffer (0.8% (w/v) NH_4Cl, 0.084% (w/v) $NaHCO_3$ and 0.038% (w/v) Na_2-EDTA, pH 7.4), incubated for 2 min at room temperature, and further diluted with PBS-1% (w/v) glucose when the parasite density was above 10^6 cells/ml. Parasites were counted under an inverted microscope using a Neubauer chamber. The minimum parasite density detectable by this method is about 1×10^5 cells/ml. Mice showing an impaired health status and/or a parasite load of $\geq 10^8$ cells/ml blood were euthanized. The Kruskal-Wallis test (followed by Dunn's multiple comparison) and the log rank test were applied to assess statistical significance of the parasitemia and the Kaplan-Meier survival plots, respectively, using GraphPad Prism version 6.01 for Windows (GraphPad Software, La Jolla, California, USA).

2.11. Production of recombinant cysteine mutants of Grx2

To generate Grx2 mutants in which Cys34 or both Cys31 and Cys34 were replaced by serine, the pETtrx1b/*grx2* plasmid [9] was subjected to site-directed mutagenesis as outlined above for the pHD1700 vector. *E. coli* cells were transformed with pETtrx1b/*grx2-c34s* or pETtrx1b/*grx2-c31s/c34s* and the recombinant proteins purified as described for the authentic Grx2 [9]. The protein concentration was determined in a Bradford assay.

2.12. Enzymatic assays

The assays were performed as described previously [9]. Insulin reductase assay: In a total volume of 800 µl 100 mM potassium phosphate, 2 mM EDTA, pH 7.0, the assay mixtures contained 625 µM DTT and 130 µM insulin as well as none, 0.7 µM Tpx, 9 or 22 µM of Grx2, C34S Grx2 or C31S/C34S Grx2. The increase in turbidity was followed at 650 nm and 30 °C. HED assay: In a total volume of 1 ml 100 mM potassium phosphate, 1 mM EDTA, pH 7.0, 200 µM NADPH, 1 mM GSH, 1 U human GR, and 2.5 mM HED were incubated for 3 min at 25 °C. 400 nM of the different Grx2 species was added and NADPH consumption followed at 340 nm.

2.13. Determination of the cellular redox state of Grx2 under standard and stress conditions

To establish the procedure, 200 µM recombinant WT, C34S or C31S/C34S Grx2 in 50 µl of 50 mM Tris/HCl, 1 mM EDTA, 1% w/v SDS, pH 7.5 (reaction buffer) was incubated for 20 min at 50 °C with 10 mM DTT. 50 µl of 60 mM AMS in reaction buffer was added. The samples were incubated for 1 h at 37 °C and then subjected to SDS-PAGE on a 16% gel. The proteins were visualized by Coomassie staining.

To follow the redox state of Grx2 in oxidatively stressed cells, six samples, each with 4×10^7 PC cells harvested in the logarithmic growth phase, were washed and re-suspended in 900 µl PBS. 1. Unstressed cells: (a) 100 µl of ice-cold TCA was added and the mixture kept on ice for 30 min. After centrifugation, the pellet was washed three times with 500 µl ice-cold acetone and dissolved in 100 µl reaction buffer, (b) after the TCA precipitation, the pellet was dissolved in 100 µl reaction buffer containing 30 mM AMS and the solution incubated for 1 h at 37 °C. 2. Cells treated for 5 min at RT with 3 mM diamide were processed as described under 1. 3. The diamide-stressed cells were reset to normal culture conditions and after 5 min treated as described in 1. All samples were subjected to Western blot analysis.

3. Results

3.1. In BS Trypanosoma brucei Grx2 is dispensable

RNAi towards Grx2 did not reveal any proliferation defect for BS *T. brucei* [9]. Thus, both *grx2* alleles were deleted by replacing one allele at a time by puromycin and neomycin resistance genes (Fig. S1A). PCR analysis confirmed the correct insertion of the resistance genes in the *grx2* locus and the absence of the *grx2* gene (Fig. S1B). Accordingly, Western blot analyses of total cell lysates revealed Grx2 in WT parasites but not the Grx2 KO cell line (Fig. 1A). The latter cells were then cultured in the absence of the selecting antibiotics. Western blot analysis against Grx1 did not show any difference in the protein levels between WT and Grx2 KO cells (Fig. 1B). The respective behavior was observed for Grx2 in Grx1 KO cells [49] indicating that the levels of the two dithiol Grxs in BS cells are mutually independent in accordance with their distinct cellular localization.

3.2. BS cells lacking Grx2 are less temperature-sensitive compared to WT parasites

Under standard culture conditions at 37 °C, the Grx2 KO cells proliferated like the WT control with a doubling time of about 6 h (not shown). Based on our earlier finding that cytosolic Grx1 links heat response to cell proliferation [49], we investigated the growth phenotype of the Grx2 KO cells at 39 °C. Within 5 days of continuous cultivation at 39 °C, the proliferation of WT cells gradually decreased suggesting a loss of fitness. In contrast, cells lacking Grx2 retained a significantly higher proliferation rate (Fig. 1C). To verify that the altered phenotype was due to the absence of Grx2, the Grx2 KO cells were transfected with pHD1700/*grx2* which allowed the tet-inducible expression of an ectopic copy of the protein (for details see Materials and methods). The inducible Grx2 KO cells were grown overnight at 37 °C in the absence and presence of tet and then cultured at 39 °C. The mutant cells behaved like the WT parasites independent of the presence or absence of tet (Fig. 1C). Western blot analysis revealed leaky expression of the ectopic Grx2 (Fig. 1A). Therefore, the higher proliferation rate of the Grx2-deficient cells at 39 °C can be ascribed to the specific absence of the oxidoreductase. Western blots of total lysates from WT BS parasites that were grown at 37 °C or 39 °C revealed identical Grx2 levels ruling out a putative temperature-induced upregulation of the protein (not shown).

To get an insight into the underlying cellular mechanism, WT and Grx2 KO cells were cultured for three days at 39 °C and then subjected to immunofluorescence microscopy. Kinetoplast (K, mitochondrial) and nuclear (N) DNA were visualized by DAPI staining and five different configurations of kinetoplasts and nuclei were quantified (Fig. 1D). Parasites in the G1 or mitochondrial S phase of the cell cycle possess a single kinetoplast and a single nucleus and are termed 1K1N. As the cell cycle progresses, the kinetoplast replicates and segregates before the nucleus generating a 2K1N cell. The cell then enters mitosis, the outcome of which is a 2K2N cell. Finally, cytokinesis occurs, cleaving the cell into 1K1N siblings [57]. In a standard culture of BS parasites, about 83%, 10%, and 5% of the cell population display 1K1N, 2K1N, and

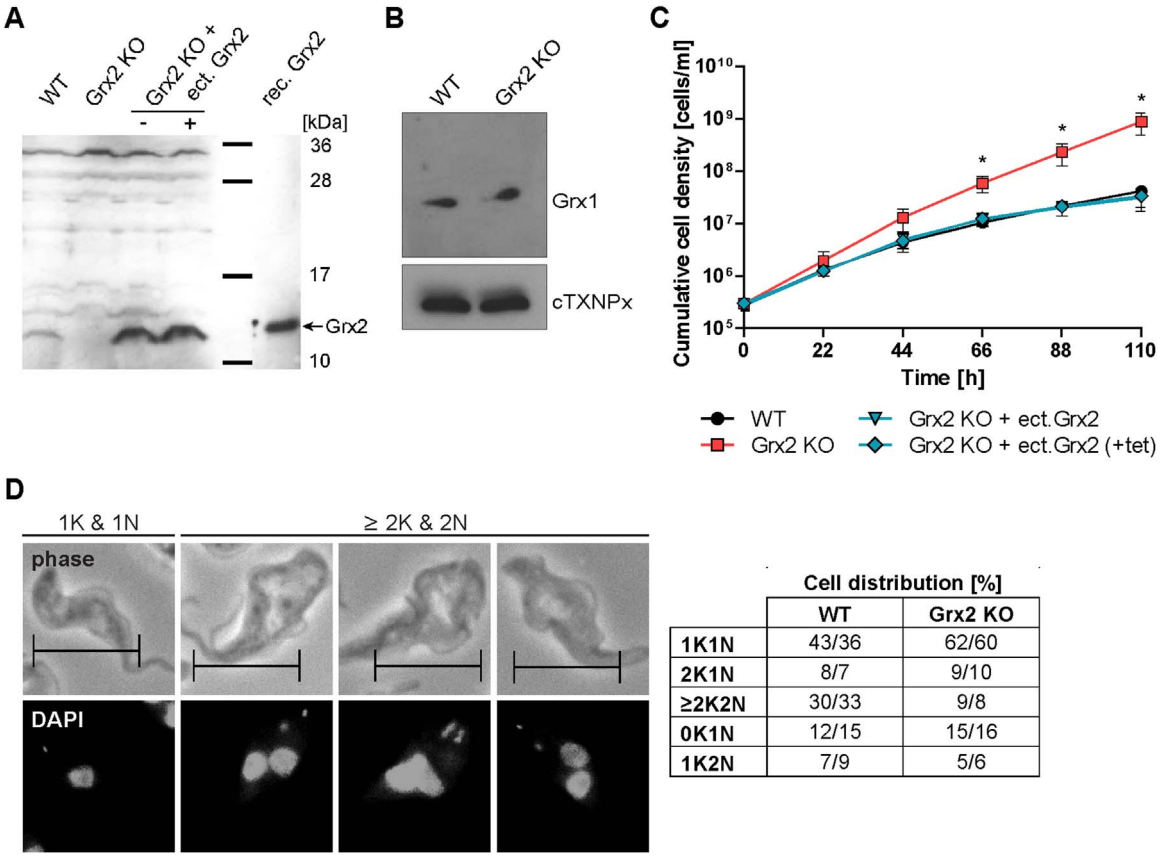

Cell distribution [%]	WT	Grx2 KO
1K1N	43/36	62/60
2K1N	8/7	9/10
≥2K2N	30/33	9/8
0K1N	12/15	15/16
1K2N	7/9	5/6

Fig. 1. Phenotypic analysis of WT and Grx2 KO BS *T. brucei* grown at 39 °C. A. Total lysates from 3 × 10^7 WT, Grx2 KO, and inducible Grx2 KO cells grown under normal culture conditions at 37 °C in the absence (-) and presence (+) of tet as well as 5 ng recombinant Grx2 were subjected to Western blot analysis with rabbit Grx2 antibodies. B. Total lysates from 1 × 10^7 WT and Grx2 KO cells grown under normal culture conditions at 37 °C were subjected to Western blot analysis with antibodies against Grx1 followed by antibodies against cytosolic 2-Cys-peroxiredoxin (cTXNPx) as loading control. There was no upregulation of Grx1 in the Grx2 KO cell line compared to the WT control. C. WT, Grx2 KO and Grx2 KO cells harboring a tet-inducible ectopic copy of *grx2* were seeded at a density of 2 × 10^5 cells/ml in 5 ml of 39 °C pre-warmed HMI-9 medium and cultured at 39 °C. The inducible Grx2 KO cells were grown in the absence and presence of 1 μg/ml tet. Every 22 h, living cells were counted and the cultures diluted back to the initial cell density. The graph shows the cumulative cell densities for the different cell types derived from three independent experiments. The mean ± standard deviation is depicted where * indicates p-values < 0.05 (calculated using Microsoft Excel Student's unpaired *t*-test with equal variance). The inducible Grx2 KO cells behaved like WT controls independent of tet due to leaky expression of the ectopic copy (see A). D. WT and Grx2 KO cells cultured for three days at 39 °C were harvested and subjected to fluorescence microscopy using DAPI to stain the kinetoplast (K, small dot) and nuclear (N, large dot) DNA. Representative WT cells are depicted. Phase, phase contrast pictures (scale bar 10 μm). At least 200 parasites of both cell types were scored for their number of kinetoplasts and nuclei and the percentage of cells displaying the respective phenotype was calculated. The results from two independent experiments are presented.

2K2N configuration, respectively [60]. Subjecting BS cells to 39 °C shifted the distribution dramatically. As noted previously [49], the proportion of WT parasites with 1K1N was lowered by 50% compared to cultivation at 37 °C and cells with ≥ 2K2N increased to ≥ 30% (Fig. 1D). In addition, many cells appeared to be fused and bearing two flagella suggesting that cytokinesis initiates but is unable to complete (Fig. 1D, upper part). In contrast, with 61% 1K1N and ≤ 9% 2K2N, Grx2 KO cultures grown at 39 °C displayed a distribution more similar to WT cells cultured at 37 °C. Other configurations such as cells with 0K1N and 1K2N, which are undetectable under standard conditions [57,60], occurred in both cultures and may be the result of unsymmetrical division of the kinetoplast or failure to segregate at all [38,57]. When put back to 37 °C, both WT and Grx2 KO cells readily resumed normal growth. This indicates that the temperature rise induced a reversible proliferation arrest but did not affect cell viability. Remarkably, BS *T. brucei* that lack the cytosolic Grx1 display an almost identical phenotype at 39 °C [49]. This suggests the presence of one or more step(s) involved in the cell cycle/proliferation response of BS cells to elevated temperatures that is/are susceptible to Grx-mediated redox control.

3.3. An elevated culture temperature does not affect the subcellular localization of Grx2

The primary structure of Grx2 does not display any obvious targeting signal. In the insect stage, subcellular fractionation indicated a localization in the mitochondrial IMS [9] (see also Fig. 9). To assess the localization of Grx2 in the BS form of *T. brucei*, the parasites were treated with increasing concentrations of digitonin which results in the gradual permeabilization of cellular membranes [9,14]. Western blot analysis of the supernatant and pellet fractions of each sample revealed the cytosolic marker protein cTXNPx completely solubilized at a digitonin: protein ratio of 0.1:1 (mg/mg) whereas the mitochondrial matrix protein LipDH appeared in the supernatant at a ratio of 0.4:1 (Fig. S2A). Grx2 remained in the pellet fraction up to a digitonin: protein ratio of 0.2:1, indicating that the protein does not occur in the cytosol. Solubilization of Grx2 started at a ratio of 0.3:1, slightly earlier than LipDH in accordance with a mitochondrial, putatively IMS localization.

To evaluate if the temperature increase affected the cellular distribution of Grx2, BS cells were grown at 39 °C for two days and then subjected to fractionated digitonin lysis (Fig. S2B). The elution pattern of cTXNPx remained unchanged and was identical with that of Tpx, another cytosolic marker. Also the elution pattern of Grx2 was identical in cells grown at 37 °C or 39 °C indicating that the protein retained its subcellular localization. LipDH and mtTXNPx were completely

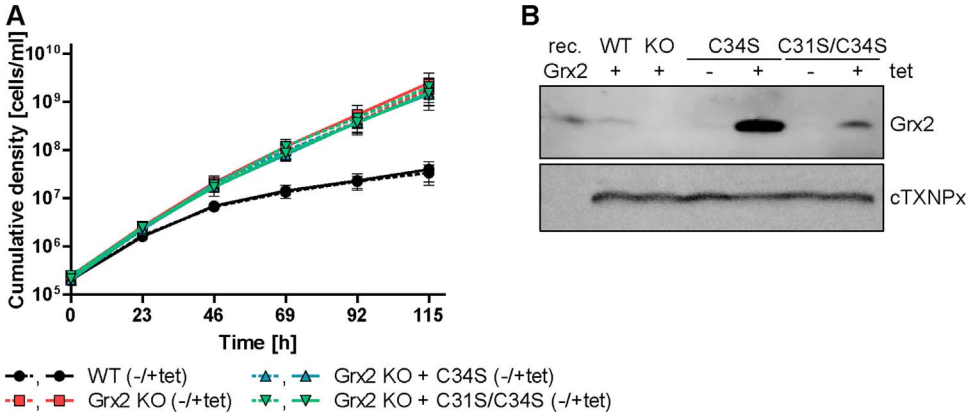

Fig. 2. Cysteine mutants of Grx2 are unable to restore the temperature sensitivity of WT BS cells. A. BS WT, Grx2 KO, and Grx2 KO cells that allowed the inducible expression of the C34S or C31S/C34S mutant of Grx2 were grown ± tet at 39 °C. Living parasites were counted every 23 h and the cultures were diluted to the initial density of 2×10^5 cells/ml. The data represent the mean ± standard deviation of three independent experiments. B. Total lysates of 2×10^7 cells harvested after 48 h cultivation at 39 °C were subjected to Western blot analysis against Grx2 (guinea pig, 1:500) and cTXPNx (1:2000) as loading control. Rec. Grx2, 5 ng recombinant protein.

solubilized at a digitinin: protein ratio of 0.5:1. Intriguingly, a minor but constant fraction of the mitochondrial matrix proteins was found in the supernatants at low digitonin concentrations suggesting that the elevated temperature affected the integrity of the mitochondrion.

3.4. The temperature sensitivity of BS WT T. brucei requires Grx2 with both active site cysteines

As shown in Fig. 1, when cultured at 39 °C, WT cells displayed a strong growth retardation whereas the Grx2 KO cells continued to proliferate. This growth advantage was abolished when the Grx2 KO cells expressed an ectopic copy of the authentic protein. To examine if the contribution of Grx2 to this growth phenotype is redox-dependent, the Grx2 KO cells were complemented with constructs that allowed the tet-inducible expression of either the C34S or C31S/C34S mutant of Grx2 (for details see Materials and methods). WT parasites and the different Grx2 KO cell lines were cultured for five days at 39 °C (Fig. 2A). Interestingly, the temperature sensitivity of WT parasites was not restored when the Grx2 KO cells even over-expressed the C34S or C31S/C34S mutant (Fig. 2B). This suggests that the strong proliferation defect of BS *T. brucei* at 39 °C involves a Grx2-mediated redox-regulated step that requires both active site cysteine residues.

3.5. BS Grx2 KO and Grx1/Grx2 KO cells display an identical thermotolerance

Since the deletion of Grx2 (this work) as well as Grx1 [49] yielded BS *T. brucei* with an identical growth phenotype at 39 °C, we decided to study the biological impact of deleting both oxidoreductases. With (blasticidin resistant) BS Grx1 KO cells [49] as starting material, both *grx2* alleles were deleted by replacing one allele at a time with puromycin and neomycin resistance genes. PCR analysis confirmed the correct insertion of the resistance genes in the *grx2* locus and the absence of both *grx1* and *grx2* (Fig. S3A, Fig. 3A). Three Grx1/Grx2 KO clones as well as WT and Grx2 KO cells were then cultured for five days at 39 °C (Fig. S3B and Fig. 3B). Whereas after three days, the WT parasites virtually stopped proliferation (see also Figs. 1C and 2A), the mutant cell lines continued to grow. No difference was observed between the Grx2 KO and Grx1/Grx2 KO cell lines suggesting that the two oxidoreductases are not redundant but act in series within a common redox-regulated pathway that arrests cell proliferation at elevated temperatures.

3.6. Growth at 39 °C shifts the cellular thiol status of BS T. brucei to more oxidizing conditions

The finding that a redox-active form of Grx2 is required to overcome the thermotolerance of Grx2-deficient BS cells suggested that the temperature shift may affect the cellular thiol redox homeostasis. To assess if the temperature rise has an effect on the cellular GSH, Gsp and $T(SH)_2$ pool, the thiols were derivatized with mBBr and quantified by HPLC analysis as described before [64]. BS WT *T. brucei* that were cultured under standard conditions at 37 °C had about 350 µM $T(SH)_2$, 100 µM GSH and 10 µM Gsp. In addition, the levels of the free thiols and free thiols plus disulfides were almost identical indicating that all three thiol species were exclusively present in free and reduced form (Fig. 4A, left graph). The values were in perfect agreement with our previously published data [64]. Cultivation of BS parasites at 39 °C altered the cellular thiol redox balance, resulting in a slight decrease of the GSH level and undetectable Gsp level which might suggest a slight shift to $T(SH)_2$ formation. Most remarkably, a significant portion of the cellular trypanothione was now in the disulfide form (Fig. 4A, right graph). As shown in Fig. 4B, at both temperatures, the Grx1/Grx2 KO cells showed virtually the same pattern as WT cells.

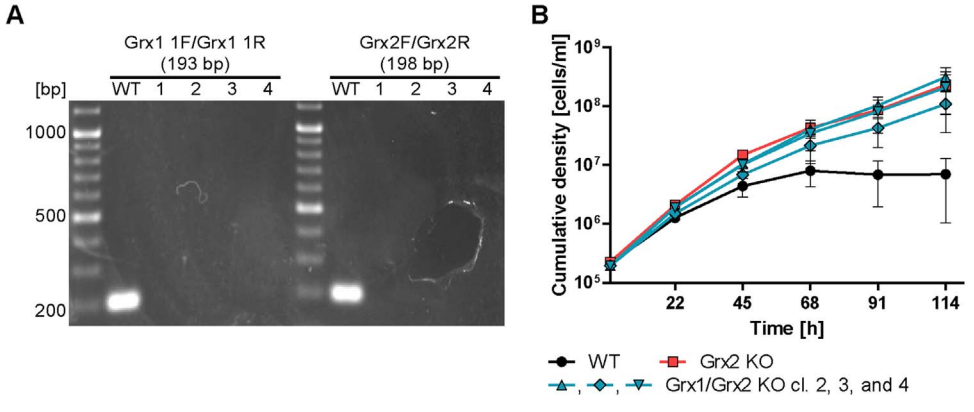

Fig. 3. Generation and temperature behavior of BS *T. brucei* lacking both Grxs. A. PCR analysis of genomic DNA isolated from WT *T. brucei* and four Grx1 KO cell lines (1 – 4) transfected with constructs to replace the *grx2* alleles by puromycin and neomycin resistance genes. Internal primers for Grx1 and Grx2 were used to demonstrate the absence of any *grx1* and *grx2* allele. The primer combinations with the expected amplicon sizes in brackets are given above each lane. The primer sequences are shown in Table S1. B. WT, Grx2 KO, and Grx1/Grx2 KO cells (clones 2, 3, and 4) were seeded at a density of 2×10^5 cells/ml in 5 ml of 39 °C pre-warmed medium and cultured at 39 °C. Every 22 h or 23 h, the cells were counted and diluted to the initial cell density. The graph shows the cumulative cell densities of the different cell types. The data represent the mean ± standard deviation of three independent experiments.

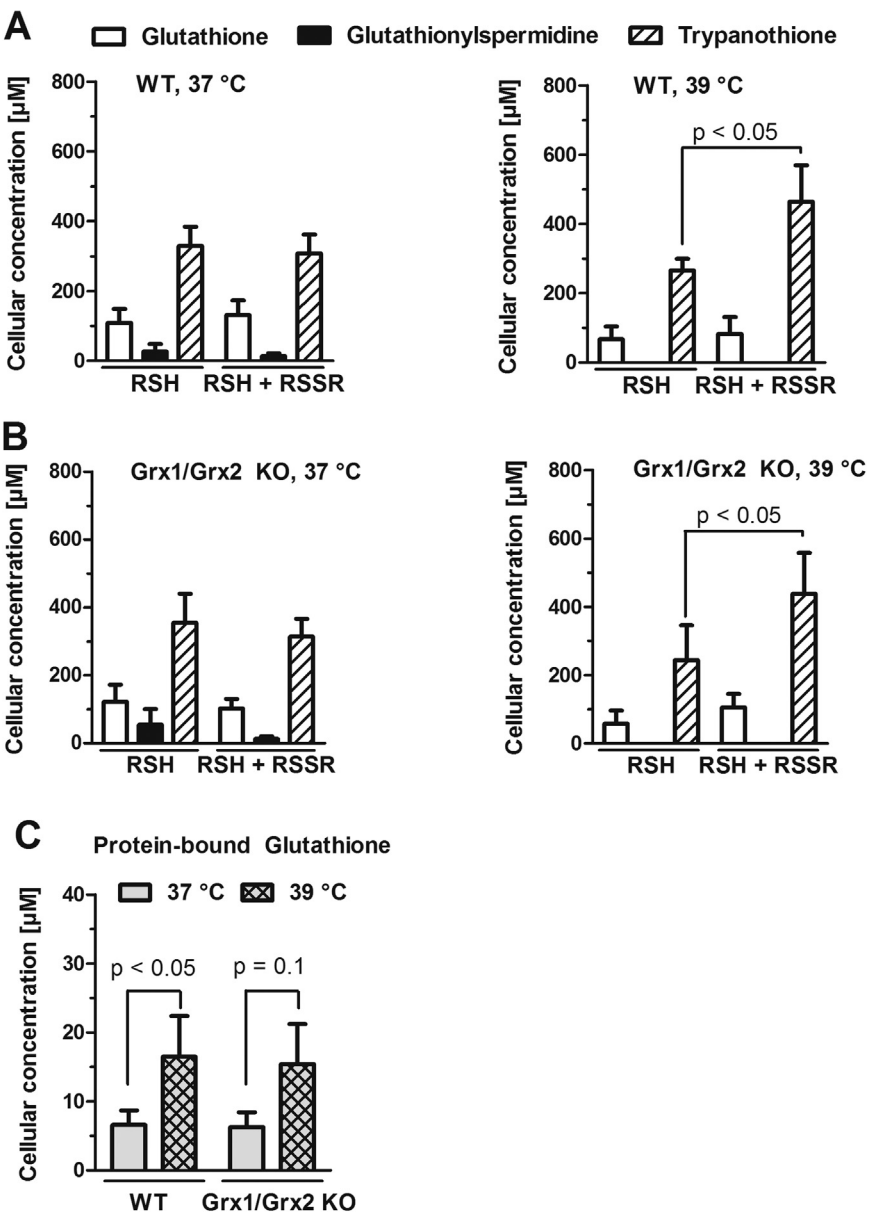

Fig. 4. Upon cultivation at 39 °C, BS WT and Grx1/Grx2 KO cells show an increase in trypanothione disulfide and protein-bound glutathione. A. WT parasites grown for 48 h at 37 °C or 39 °C were counted and immediately lysed by TCA precipitation. Half of the supernatant was directly reacted with mBBr to label the free thiols (RSH). The other half was treated with TCEP, followed by mBBr, yielding the sum of free thiols and disulfides (RSSR). B. Grx1/Grx2 KO cells were analyzed as described under A for the WT parasites. **C.** The TCA pellet was dissolved in buffer containing TCEP and the released thiols were labeled with mBBr. The thiol derivatives were separated and quantified by HPLC analysis. For details see Material and methods. The values are the mean ± SD of at least three independent analyses.

Another remarkable effect induced by this minor (2 °C) temperature shift was the increase in the level of S-glutathionylated proteins (from ~7 µM to ~17 µM) in both WT and Grx1/Grx2 KO cells (Fig. 4C). In summary, under this experimental setting that mimics fever in the mammalian host and generates an endogenous redox unbalance, the dithiol Grxs do not contribute to the overall GSH/GSSG and GSH/protein-SSG redox state of these cells as initially expected [12].

3.7. Lack of the dithiol Grxs does not sensitize BS cells towards oxidants

As shown above, the dithiol Grxs do not appear to be involved in the maintenance of the cellular thiol redox homeostasis when the oxidative stress originates from an increase in temperature. Nonetheless, the oxidoreductases may be part of a more general protection mechanism against an acute oxidative stress. To test this hypothesis, WT and Grx1/Grx2 KO BS *T. brucei* were subjected to a short term exposure to hydrogen peroxide, diamide as well as arsenicals, all of which affect the thiol redox homeostasis but *via* distinct mechanisms. For instance, hydrogen peroxide shifts the cellular GSH and $T(SH)_2$ to the free disulfide forms whereas in diamide-treated cells the main products are S-glutathionylated and S-trypanothionylated proteins [64]. Arsenicals form stable complexes with $T(SH)_2$ and inactivate trypanothione reductase [16,20]. To exclude any interaction between the reagents and thiols in the culture medium, the cells were transferred into HMI-9 medium lacking cysteine and 2-ME and then treated with hydrogen peroxide, diamide or sodium arsenite (Fig. S4). The concentrations of the reagents were chosen to mildly or severely affect the viability of WT cells. Every hour, living cells were counted. During the five hours observation time, unstressed control cells even slightly proliferated indicating that the thiol-depleted medium did not impose an additional stress. Towards all three stressors, the Grx1/Grx2 KO cells displayed the same behavior as the WT controls. This clearly shows that in infective *T. brucei* the dithiol Grxs are not involved in the protection against acute oxidative stress.

3.8. The dithiol Grxs are fully dispensable for infectivity and parasite survival in a mammalian host

In vitro proliferation does not resemble the more challenging conditions parasites face during host infection and, hence, may hide a detrimental phenotype as shown for BS *T. brucei* lacking the mitochondrial LipDH [58]. Thus, in order to provide compelling evidence for the biological role of the dithiol Grxs in infectious trypanosomes,

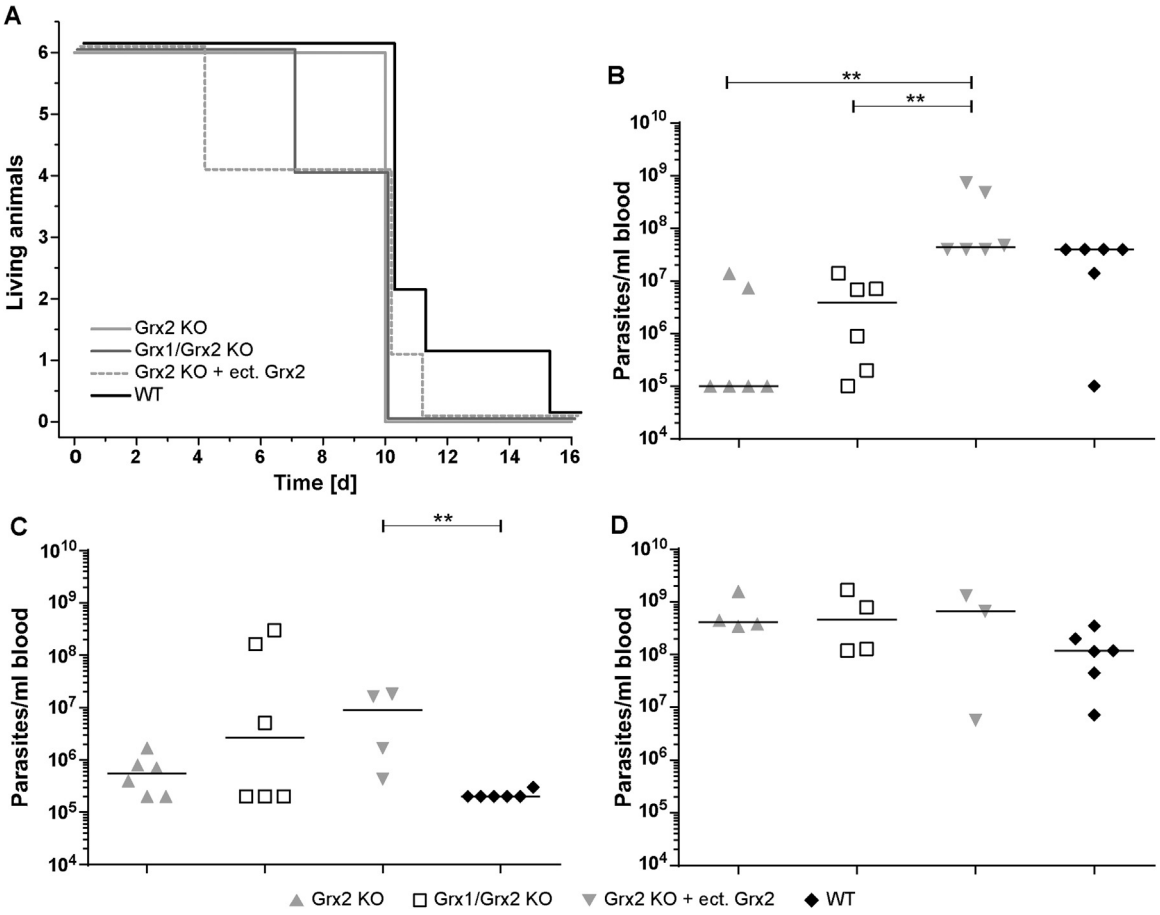

Fig. 5. Infectivity of Grx2 KO, Grx1/Grx2 KO and Grx2 KO cells expressing an ectopic copy of Grx2 as well as WT *T. brucei*. Female BALB/cJ mice (n = 6/group) were infected intraperitoneally with 10^4 parasites. A. Kaplan-Meier survival plot of mice infected with the respective cells. The plots are slightly displaced to allow a better visualization. B-D. Parasite load in blood samples from infected animals taken at (B) day 4, (C) day 7, and (D) day 10 post-infection. The horizontal bars represent median values and ** denotes statistically significant differences with a p-value of < 0.01.

mice (n = 6/group) were infected with WT, Grx2 KO, Grx2 KO cells expressing ectopically Grx2 and Grx1/Grx2 KO cells, respectively, and animal survival and parasitemia recorded (Fig. 5). Although early animal death (n = 2) occurred at day 4 and 7 post infection with Grx2 KO cells ectopically expressing Grx2 and Grx1/Grx2 KO cells, respectively, no significant differences were observed between the distinct groups which all shared a mean survival time of 10 days (Fig. 5A). The parasitemia in the group infected with WT parasites displayed the typical trend earlier described for infections with monomorphic parasites [26,45,49,58]. After a peak at day 4 (Fig. 5B), parasite proliferation is largely controlled by the host at day 7 (Fig. 5C), which parallels the immune response of the host [42], and finally ends in an uncontrolled multiplication ($\geq 10^8$ parasites/ml blood at day 10; Fig. 5D) and animal death (Fig. 5A). For the groups infected with the mutant cell lines, the parasitemia presented an overall similar, but not identical picture. In particular, at day 4, the Grx2 KO and Grx1/Grx2 KO cells were significantly less proliferative than the Grx2 KO cells that ectopically expressed Grx2 (Fig. 5B). At day 7, animals infected with the latter cells presented a significantly higher parasitemia compared to those infected with WT parasites (Fig. 5C) which suggests that they have a higher capacity to adapt to and withstand the innate immunity of the murine host during the early stage of infection. The *in vivo* phenotype of these cells may be associated with their much higher Grx2 content compared to WT cells (Fig. 1A). We do, however, not know if the overexpressed protein is correctly transferred to its physiological site or largely remains in the cytosol. In summary, our data show that the infective form of African trypanosomes does not require dithiol Grxs to establish infection and survive in a mammalian host.

3.9. PC T. brucei are refractory to deletion of both grx2 alleles and require a redox active Grx2 species for viability

To provide conclusive evidence that Grx2 is indispensable in PC cells, the *grx2* alleles were replaced by transfection with puromycin and neomycin resistance cassettes. Resistant cell lines were cloned as depicted schematically in Fig. S1 for BS cells. Both transfections yielded at least three SKO cell lines. However, attempts to replace the second allele failed. Only a single double-resistant cell line was obtained but PCR analysis still revealed the presence of a *grx2* copy (Fig. S5A). Both the Grx2 SKO clone and the double resistant cell line displayed a lower Grx2 level compared to WT cells (Fig. S5B). Supporting previous findings that depletion of the Grx2 mRNA results in a proliferation defect of PC cells [9], the Grx2 SKO parasites displayed a slightly but significantly lower growth rate compared to WT cells (Fig. S5C). Strikingly, after several months in culture, this minor proliferation defect was lost (not shown) and Western blot analysis revealed that the Grx2 SKO clone cells had recovered a Grx2 level comparable to that in WT cells (Fig. S5D).

Based on the finding that Grx2 is essential for the proliferation of PC *T. brucei*, we aimed at elucidating if this requires a redox-active form of the protein. For this purpose, a Grx2 SKO cell line (puromycin resistant) was transfected with hygromycin-resistance constructs that allow the ectopic expression of WT, C34S, and C31S/C34S Grx2, respectively. The cells were cultured in the presence of tet to induce expression of the respective protein species, and then transfected with the neomycin resistance cassette to replace the second *grx2* allele. Stably-transfected clones were selected by serial dilutions in medium containing

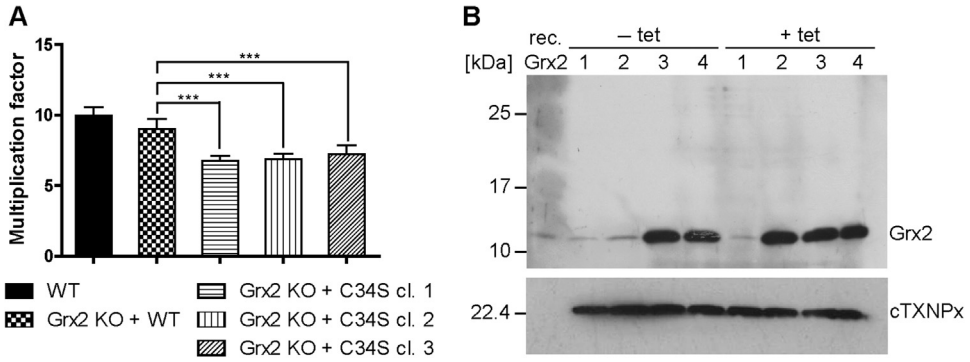

Fig. 6. PC Grx2 KO cells that express C34S Grx2 show a slightly impaired growth when compared to WT or Grx2 KO cells ectopically expressing authentic Grx2. A. WT parasites, Grx2 KO cells that harbored an ectopic copy of WT Grx2 and three clones of Grx2 KO cells with an ectopic copy of C34S Grx2 were seeded at a density of 5×10^5 cells/ml and grown for five days in the presence or absence of tet. Every 22 h, the cells were counted and the cultures diluted back to the initial density. The average multiplication factor for the different cells was calculated for all 22 h intervals. Since for each individual cell line, the proliferation rate at all time points as well as in the presence or absence of tet was virtually identical, the values were combined. The data are the mean ± standard deviations of three individual experiments. Significant differences are indicated by *** (p-value ≤ .001, calculated using Microsoft Excel Student's unpaired t-test with equal variance). B. At each time point, an aliquot of the culture was withdrawn. Shown here is a representative Western blot with total lysates from 1.4×10^7 cells harvested after 88 h and loaded onto a 14% SDS gel. rec. Grx2, 5 ng recombinant Grx2. 1, WT cells, 2 and 3, Grx2 KO cells expressing the C34S mutant (clone 2 and 3, respectively), and 4, Grx2 KO cells expressing an ectopic copy of WT Grx2, grown in the absence (-) or presence (+) of tet. The membrane was developed with rabbit Grx2 antibodies and then re-probed for cTXNPx as loading control. Independent of tet, the conditional KO cell lines expressed the respective Grx2 species at least at the level of the authentic protein in WT cells.

hygromycin, tet, puromycin and G418. Parasites with both *grx*2 alleles replaced were obtained only if an ectopic copy of *grx2* or *grx2-c34s* – but not *grx2-c31s/c34s* – had been integrated into the genome as confirmed by PCR analysis (Fig. S6).

The growth phenotype of WT *versus* Grx2 KO cell lines ectopically expressing either WT or C34S Grx2 was followed for five days. Grx2 KO cells that harbored an ectopic copy of authentic *grx2* proliferated like the WT control. In comparison, all three cell lines expressing the C34S mutant displayed a slightly slower proliferation (Fig. S7) which mirrored their significantly diminished multiplication factors (Fig. 6A). Growth of all inducible Grx2 KO cell lines was independent of tet. This was due to leaky expression of the ectopic protein species in the non-induced cell lines which, as assessed by Western blot analysis, reached levels similar to or higher than that of endogenous Grx2 in WT cells (Fig. 6B). Overall, the data indicated that PC *T. brucei* require a redox active form of Grx2 whose biological function(s) depend to a great extent on the N-terminal active site cysteine.

3.10. Recombinant Grx2 lacking Cys34 retains deglutathionylation activity

To get a deeper insight in the reaction type catalyzed by the C34S mutant, and thus to infer the putative biological function of Grx2 in PC cells, the recombinant protein was subjected to different enzymatic assays. Insulin reduction is catalyzed very efficiently by thioredoxins, oxidoreductases operating *via* a dithiol/disulfide exchange mechanism [27]. Some Grxs accelerate the reaction as well, although with much lower efficiency. In accordance with previous data [9], recombinant *T. brucei* Tpx and Grx2 catalyzed the reduction of insulin. In contrast, the C34S mutant of Grx2 did not show any activity (Fig. 7A).

The HED assay is the most commonly used Grx-specific assay [40]. HED reacts spontaneously with GSH yielding 2-ME and the mixed disulfide between 2-ME and GSH (2-ME-SSG), which then acts as substrate of Grx. The Grx-catalyzed reaction frees the second 2-ME molecule and generates a mixed disulfide between GSH and the N-terminal active site cysteine of Grx. This glutathionylated form (Grx-SSG) is resolved by attack of a second GSH molecule yielding reduced Grx and glutathione disulfide (GSSG) [5]. The overall reaction is monitored as consumption of NADPH in the glutathione reductase-catalyzed reduction of GSSG. Recombinant C34S Grx2 catalyzed HED reduction with about 40% activity compared to WT Grx2 (Fig. 7B). As expected, the double cysteine mutant (C31S/C34S) of Grx2 lacked HED activity as the absorption decrease was only marginally higher than that of the spontaneous reaction in the absence of Grx. Since C34S Grx2 had a lower activity than the authentic protein, one might expect that upon overexpression the mutant should restore WT proliferation. However, this was not the case (see Fig. 6) possibly because the overexpressed protein remained largely in the cytosol. Taken together, the essential function of Grx2 in PC *T. brucei* can follow a monothiol mechanism such as, for instance, the reduction of protein-SSG mixed disulfides.

3.11. Cellular Grx2 is in the fully reduced state and susceptible to reversible oxidation but is not involved in protection against exogenous oxidative stress

Next we asked for the physiological redox state of Grx2. Labeling of a cysteine residue with AMS causes a mass increase of 500 Da. Grx2 possesses only two cysteine residues which form the active site CQFC motif. To verify the accessibility and reactivity of the residues in the folded protein, recombinant WT Grx2 and cysteine mutants were treated with DTT followed by excess AMS and then subjected to SDS-PAGE and Coomassie staining. WT, C34S and C31S/C34S Grx2 displayed a shift that corresponded to the incorporation of two, one and no AMS label, respectively (Fig. 8A) demonstrating that the procedure is suitable to evaluate the cellular redox status of Grx2.

Diamide is a strong disulfide-inducing reagent [32] that in different cell types induces protein S-thiolation [37,64]. To mimic an oxidative stress condition sensed by Grx2, PC *T. brucei* were exposed for five min to 3 mM diamide, or diamide-stressed and reset for five min to normal medium or kept under standard culture conditions (control). The cells were harvested by TCA precipitation. The proteins were re-dissolved, treated with AMS and subjected to Western blot analysis. For the control cells, the AMS treated sample displayed a complete shift of the protein band indicating that Grx2 is in the fully reduced state (Fig. 8B, lanes 1 and 2). In contrast, in diamide-stressed parasites, the running behavior of Grx2 was unaffected (lanes 3 and 4) in accordance with formation of the intramolecular disulfide which prevented any reaction with the thiol reagent. Five min after re-transferring the stressed cells into normal medium, Grx2 reacted again with two AMS molecules and thus was in the fully reduced state (lanes 5 and 6). Taken together, under physiological conditions, cellular Grx2 is present completely in the dithiol state. Upon challenging PC cells with a strong oxidative agent, the oxidoreductase forms an intramolecular disulfide which is rapidly re-reduced after stress removal.

The finding that a redox active Grx2 is required for the proliferation of PC cells led us to question if in this life cycle stage, the protein might be involved in protection or repair mechanisms against oxidative insults. Since PC Grx2 KO cells could not be obtained, tet-inducible RNAi cell lines available from previous work [9] were used for the analysis. Depletion of the Grx2 mRNA was induced for 72 h which resulted in virtually undetectable levels of the protein and a proliferation arrest (see Fig. 10). Induced and non-induced Grx2 RNAi cells as well as WT parasites were then treated with 500 µM or 1 mM H_2O_2 and 30 µM or 60 µM diamide. The concentrations of the oxidants were chosen to exert

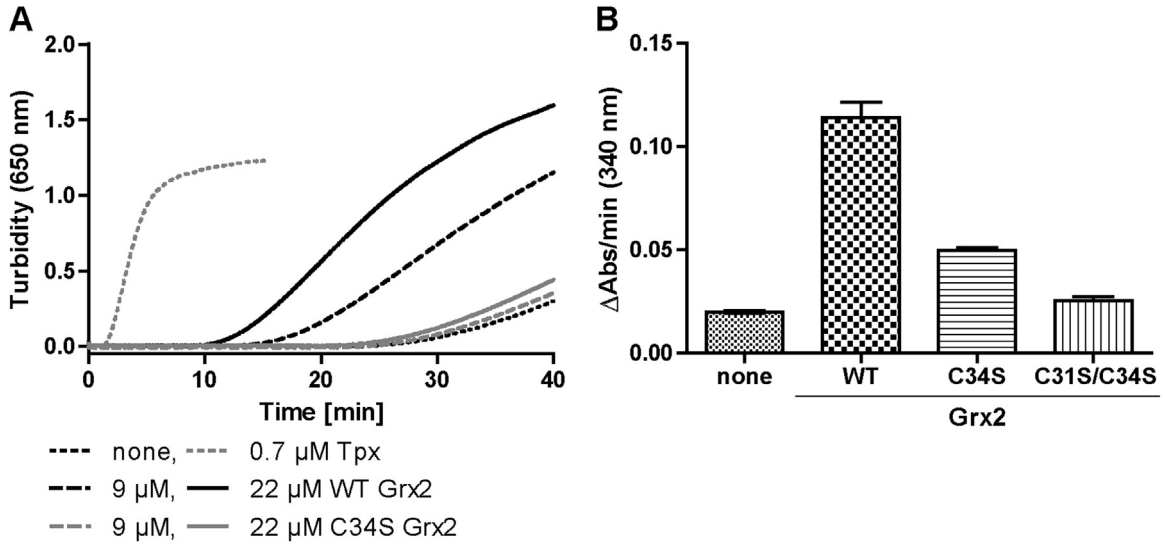

Fig. 7. Catalytic activities of Grx2 Cys-mutants. A. Insulin reduction assay. In 100 mM potassium phosphate, 2 mM EDTA, pH 7.0, the reaction mixtures contained 625 µM DTT and 130 µM insulin and either no oxidoreductase (none), Tpx, WT Grx2 or C34S Grx2 at the indicated concentrations. The increase in turbidity due to the precipitation of the insoluble beta-chain of insulin was followed at 30 °C. The data are representative for three independent experiments. B. HED assay. In a total volume of 1 ml of 100 mM potassium phosphate, 1 mM EDTA, pH 7.0, 200 µM NADPH, 1 mM GSH, 1 U of human GR and 2.5 mM HED were incubated for 3 min at 25 °C. The reaction was started by addition of 400 nM of WT, C34S and C31S/C34S Grx2, respectively. NADPH consumption was followed at 340 nm. The data are the mean ± standard deviation of three independent experiments.

either a minor or a strong effect on the WT parasites. For a total of six hours, every h as well as after 24 h, living cells were counted. As shown in Fig. S8, no significant differences were observed between the three cell types. Thus, neither in the mammalian BS nor the PC insect form of *T. brucei*, Grx2 seems to play a role in the defense against exogenous oxidative stresses.

3.12. Grx 2 is located in the mitochondrial intermembrane space of PC cells

The identification of proteins in discrete regions of the cells such as the IMS can be challenging. To get a final proof that Grx2 resides in the IMS, we used a method that combines selective cell permeabilization at 4 °C with a gel shift assay. Since AMS proved to be unsuitable because of its low solubility at 4 °C, MM(PEG)12 was used. The compound is membrane impermeable but can access the IMS by pores in the outer membrane [30]. MM(PEG)12 irreversibly alkylates cysteine residues thereby adding a molecular mass of 700 Da per moiety. PC *T. brucei* were treated at 4 °C with low and high concentrations of digitonin and the resulting pellet and supernatant fractions treated with TCEP followed by MM(PEG)12. After stopping the alkylation with 2-ME, the samples were analyzed by Western blotting with antibodies against Grx2 as well as cytosolic Tpx and the mitochondrial matrix protein ASCT [56]. All three proteins possess cysteine residues which are able to react with MM(PEG)12 and thus undergo a mass shift detectable in the Western blot.

At a digitonin: protein ratio of 0.1:1, both Grx2 and ASCT remained in the pellet fraction whereas the cytosolic Tpx was virtually completely solubilized and shifted in the MM(PEG)12-treated sample (Fig. 9). That in the absence of digitonin, MM(PEG)12 could partially modify Tpx in the pellet fraction is probably due to some damage of the cell membrane during the extensive washing and incubation steps of the pellet. The absence of the protein in the supernatant of the digitonin-free samples clearly ruled out any direct lysis of the cells. Notably, in the pellet fraction, Grx2 – but not ASCT – displayed a mass shift when the 0.1:1 sample was treated with MM(PEG)12. This shows that Grx2 was accessible although the inner mitochondrial membrane was intact. ASCT became only solubilized at the high digitonin: protein ratio (0.55:1) and then also displayed a shift upon MM(PEG)12 treatment. Taken together, Grx2 and ASCT required a high digitonin concentration for solubilization in accordance with their mitochondrial localization. In contrast to the matrix protein ASCT, Grx2 was accessible to MM(PEG)12 alkylation in the pellet fraction. This strongly suggests that Grx2 is specifically localized in the IMS.

3.13. Grx2-depleted PC cells do not show a heat phenotype but advanced proliferation under high glucose conditions

Based on the fact that Grx2 is involved in the temperature adaptation of BS *T. brucei*, a similar putative role was investigated in PC cells. Grx2 RNAi was induced for 24 h. Subsequently induced and non-induced cells as well as WT parasites were incubated at 37 °C. Within the first and second day at 37 °C, WT and non-induced cells multiplied about 10- and 5-fold, respectively, in comparison to a continuous 12-fold multiplication at 27 °C (Fig. S9). Longer incubation at 37 °C caused significant cell death. The induced Grx2 RNAi cell lines multiplied with 50% and 30% of the rate of the non-induced control (Fig. S9B).

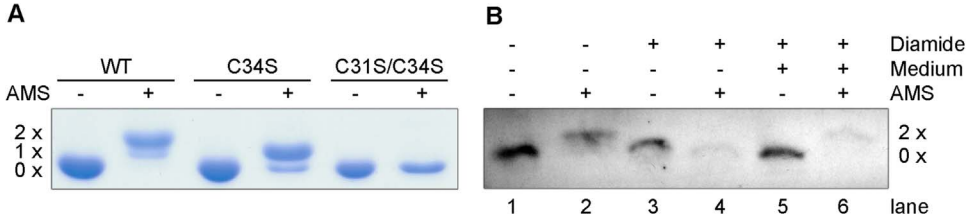

Fig. 8. Gel shift assay to reveal the cellular redox state of Grx2. A. Recombinant WT, C34S, and C31S/C34S Grx2 were treated with DTT followed by AMS as outlined in Material and methods. Each protein sample (5 µg) was subjected to SDS-PAGE and Coomassie staining. AMS adds 500 Da per modified cysteine residue. WT and C34S Grx2 showed a mass shift corresponding to two and one cysteine residue (s) alkylated by AMS, respectively. The C31S/C34S mutant does not contain any cysteine and remained unmodified. B. PC *T. brucei* were grown under normal culture conditions, stressed for 5 min with 3 mM diamide or stressed and then re-transferred for 5 min into 27 °C pre-warmed medium. Afterwards the cells were harvested and lysed by TCA precipitation. The pellet was dissolved in reaction buffer ± 30 mM AMS and incubated for 1 h at 37 °C. The extracts were subjected to Western blot analysis with rabbit Grx2 antibodies. For details see Material and methods.

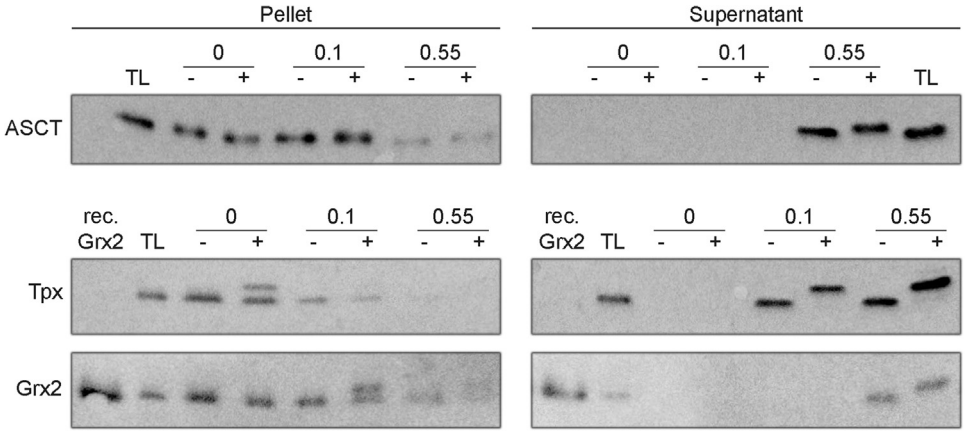

Fig. 9. Grx2 is localized in the mitochondrial IMS of PC *T. brucei*. PC parasites were treated for 4 min at 4 °C with 0, 0.1, and 0.55 digitonin/protein (mg/mg) and centrifuged. The supernatant and pellet fractions were treated with 10 mM TCEP, followed by 15 mM MM(PEG)12 (+) or the same volume of buffer (-) and the excess alkylating agent was inactivated by adding 38 mM 2-ME. Samples from 1×10^7 cells were loaded per lane on a 14% gel and subjected to Western blot analysis with Grx2 guinea pig antibodies and subsequently Tpx as cytosolic marker. In the case of the mitochondrial matrix marker ASCT, samples from 2×10^6 cells were loaded on an 8% gel. TL, total cell lysate. The analysis is a representative of four independent biological replicates.

However, an identical relative growth retardation was observed at 27 °C (Fig. S9A). Thus, Grx2 depletion affected the proliferation of PC cells but the heat-stress did not impose an additional challenge. In conclusion, in PC *T. brucei* Grx2 is essential for proliferation but most probably, the protein does not play a role in the heat-stress response.

In their natural habitat, the PC insect form of *T. brucei* dwells in the midgut of the tsetse fly, an environment poor in glucose but rich in amino acids, especially proline, and gains ATP *via* oxidative phosphorylation. However, when grown in the presence of glucose, the energy needs of the parasites can be fulfilled by substrate level phosphorylation alone [15,35]. To elucidate if the physiological role of Grx2 may be related to the activity of the respiratory chain, the Grx2-depleted cells were grown in the presence of high glucose concentrations. The MEM-Pros medium used for cultivation of PC *T. brucei* contains 5.2 mM proline but ≤ 0.5 mM glucose originating from the FCS [58,61]. To induce the metabolic adaptation to glucose consumption, WT parasites and two Grx2 RNAi clones were cultured for seven days in medium supplemented with 10 mM glucose. Control cells were kept in normal (low-glucose) medium. Subsequently, the cells were grown in the absence or presence of tet. Every 24 h, the cells were counted and the culture diluted back to the starting density of 5×10^5 cells/ml. As expected, the induced Grx2 RNAi cell lines grew at a lower rate than non-induced cells or WT parasites. However, whereas WT parasites and the non-induced cell lines proliferated at the same rate in both media, the Grx2-depleted cells retained a slightly but sustained higher growth rate in the glucose-rich medium. Fig. 10A shows for WT parasites and clone 1 the cumulative densities from three individual experiments. The higher growth rate of the Grx2-depleted cells in glucose-rich medium persisted for six days and vanished upon prolonged cultivation. An almost identical behavior was observed for clone 2 except that the effect got lost already after five days. Western blot analysis confirmed that upon RNAi induction, Grx2 was significantly down-regulated between day 1 and 6 in clone 1 (between day 2 and 5 in clone 2, not shown) and then re-appeared (Fig. 10B). The cellular Grx2 protein level was independent of the glucose concentration in the medium. For each 24 h time interval, the multiplication factor of the cells in high- and low-glucose medium was calculated and the ratio determined. In WT parasites and the non-induced clones the value was around 1 (Fig. 10C). In comparison, the induced Grx2 RNAi cells yielded higher values in the high-glucose medium. Due to some variances between the individual experiments, the clones showed statistically significant differences only at one or two time points. However, it should be pointed out that in each individual experiment (three per cell line), the Grx2-depleted cells grew better in the presence of high glucose (see Fig. S10 for an example). The data suggest that the IMS-localized Grx2 is involved in the regulation or stabilization of a respiratory chain component and thus may be less important under conditions when the cell slows down oxidative phosphorylation.

3.14. Grx2-depleted PC cells have an elongated morphology

To evaluate the reasons for the observed growth arrest of the Grx2-depleted cells, such as putative changes in the morphology and/or content of kinetoplast and nuclear DNA, the cells were treated with MitoTracker and DAPI and microscopically analyzed. Remarkably, upon RNAi induction, an increasing number of the Grx2-depleted cells displayed an elongated shape (Fig. 11A). After 72 h of RNAi induction, the mean distance between their anterior and posterior end was 17.5 ± 2.7 µm whereas in WT parasites the average total cell dimension was 15.2 ± 2.3 µm (Fig. 11B). To establish whether these changes were restricted to a specific region, the linear distances between the posterior end and the kinetoplast, between kinetoplast and nucleus, and between the nucleus and the anterior end were measured. The most prominent alteration was the mean posterior end to kinetoplast dimension which was 3.6 ± 0.9 µm in WT parasites but 4.8 ± 1.1 µm in the total population of Grx2-depleted cells. However, also the other two dimensions were increased (Fig. 11B). Both the non-induced and induced Grx2 RNAi cells showed intense MitoTracker staining indicating that Grx2-depletion does not affect the mitochondrial membrane potential. Together with the elongation of the cell body in the Grx2-depleted cells, the mitochondrion was also extended spreading from the anterior to posterior end.

To investigate if the phenotypic changes are reversible, Grx2-depletion was induced for 3 days. Afterwards the cells were either further kept in the presence of tet or transferred into tet-free medium. As expected, cells that were continuously exposed to tet proliferated at about 30% of the rate of the non-induced control culture (see Grx2 RNAi cells + tet, low glucose in Fig. S10). Cells that after 72 h RNAi induction were transferred into tet-free medium proliferated at an only marginally higher rate (not shown). This indicates that the Grx2-depleted elongated cells were unable to readapt normal proliferation.

To determine if the Grx2-depleted cells accumulated in a specific cell cycle phase, the DAPI-stained cells were assessed for their kinetoplast and nucleus content. At least 280 of each, WT, non-induced and induced Grx2 RNAi cells were inspected and the percentage of 1 K1N, 1K*1N, 2K1N, and 2K2N configuration was calculated (Fig. 11C). Cells with non-dividing kinetoplast and a single nucleus (1 K1N) are in the G1-phase. Parasites with an elongated/dividing kinetoplast (1 K*1 N) are in the mitochondrial S-phase. Trypanosomes with two kinetoplasts and 1 nucleus (2K1N) are in G2/M phase while parasites with 2K2N are post-mitotic [67]. No significant differences in the karyotypes were observed. In all three cultures about 20% of cells had a 1K*1N configuration which indicates that the Grx2-depleted cells are still able to divide the kinetoplast. Notably, of the induced Grx2 RNAi cells with 2K1N and 2K2N none had an elongated shape when compared with the respective WT parasites. Taken together, formation of the elongated morphology appears to be an irreversible step but the proliferation

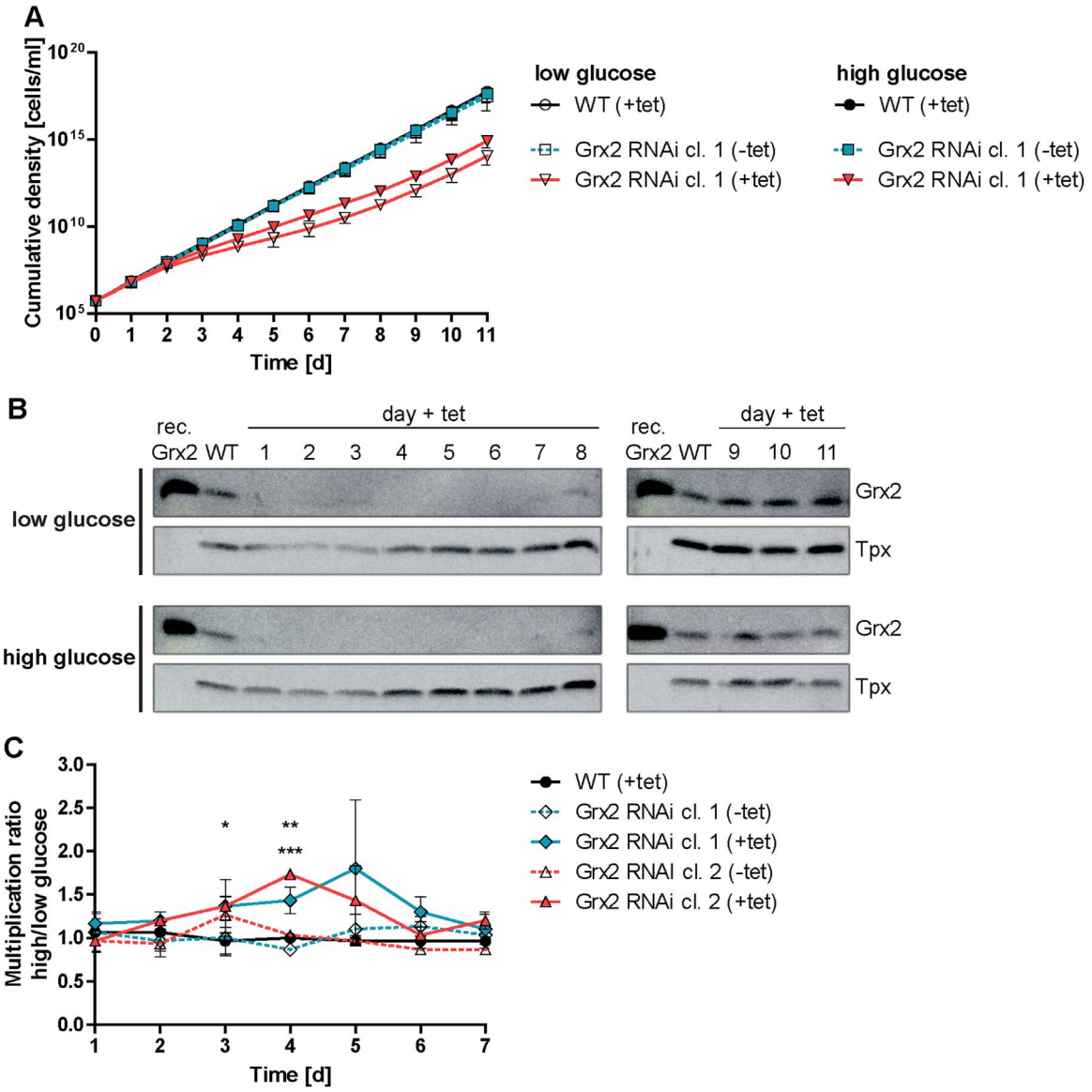

Fig. 10. Proliferation of Grx2-depleted PC parasites in glucose-rich medium. A. WT cells and two inducible Grx2 RNAi cell lines (clone 1 and 2) were cultured for seven days in normal MEM-Pros medium (low glucose) or in medium supplemented with 10 mM glucose (high glucose). Afterwards, the cells were seeded at a density of 5×10^5 cells/ml and grown in the presence or absence of tet. Every 24 h, the cells were counted and the cultures diluted back to the initial density. The cumulative cell densities are shown for WT cells and clone 1 where the values are the mean ± standard deviation from three independent experiments. The proliferation of WT parasites was unaffected by the presence of tet. Therefore only the + tet data are depicted for clarity. B. Every 24 h, a sample of the induced cells was removed. Total lysates from 1×10^7 cells (clone 1) were subjected to Western blot analysis using Grx2 guinea pig antibodies and afterwards re-probed against Tpx. rec. Grx2, 5 ng recombinant Grx2. C. For each 24 h time interval, the multiplication factor of the cells cultured ± tet and under high- and low-glucose conditions was calculated and the ratio determined. Clone 2 revealed a very similar behavior except that the protein was down-regulated only between day 2 and 5. The data are the average ± standard deviation from three independent experiments. Values > 1.0 indicate a higher proliferation rate when the cells were grown under high- *versus* low-glucose conditions. Significant differences between induced Grx2 RNAi cells and WT cells are indicated by asterisks (top: clone 1, bottom: clone 2; *, ** and *** represent p-values of < 0.05, 0.1 and 0.001, respectively).

defect of the Grx2-depleted cells does not reflect a specific cell cycle arrest.

4. Discussion

Here we report on the physiological roles the dithiol Grx2 plays in the distinct developmental stages of African trypanosomes. Grx2 is a mitochondrial protein and does not show any overlapping localization or functional redundancy with the cytosolic Grx1 [9,49]. The parasite Grx2 is a lineage-specific Grx [12,43] which localizes specifically to the IMS in contrast with the situation in mammalian or yeast cells where small sub-fractions of the cytosolic Grxs occur in the IMS [31,52]. A recent proteome approach based on the knockdown of ATOM40, the central-pore forming protein of the ATOM (archaic translocase of the mitochondrial outer membrane) complex, revealed Grx2 (but not Grx1) as one of the proteins with significantly reduced abundance upon ATOM40 RNAi induction [54]. This perfectly agrees with our localization data and indicates that Grx2 may be imported into the IMS *via* the ATOM complex.

Deletion of both *grx2* alleles did not affect the *in vitro* proliferation of BS *T. brucei*. Even parasites that lacked both Grx1 and Grx2 did not show any altered growth phenotype under standard culture conditions and had identical sensitivity towards exogenous hydrogen peroxide, diamide or arsenite when compared with WT cells. This contrasts with the situation in yeast where Grx1- or Grx2-deficient strains display a distinct pattern of sensitivity against different oxidative stressors [39]. Thus, none of the dithiol Grxs plays a crucial role in protecting infective trypanosomes against exogenous oxidative stressors. Most probably,

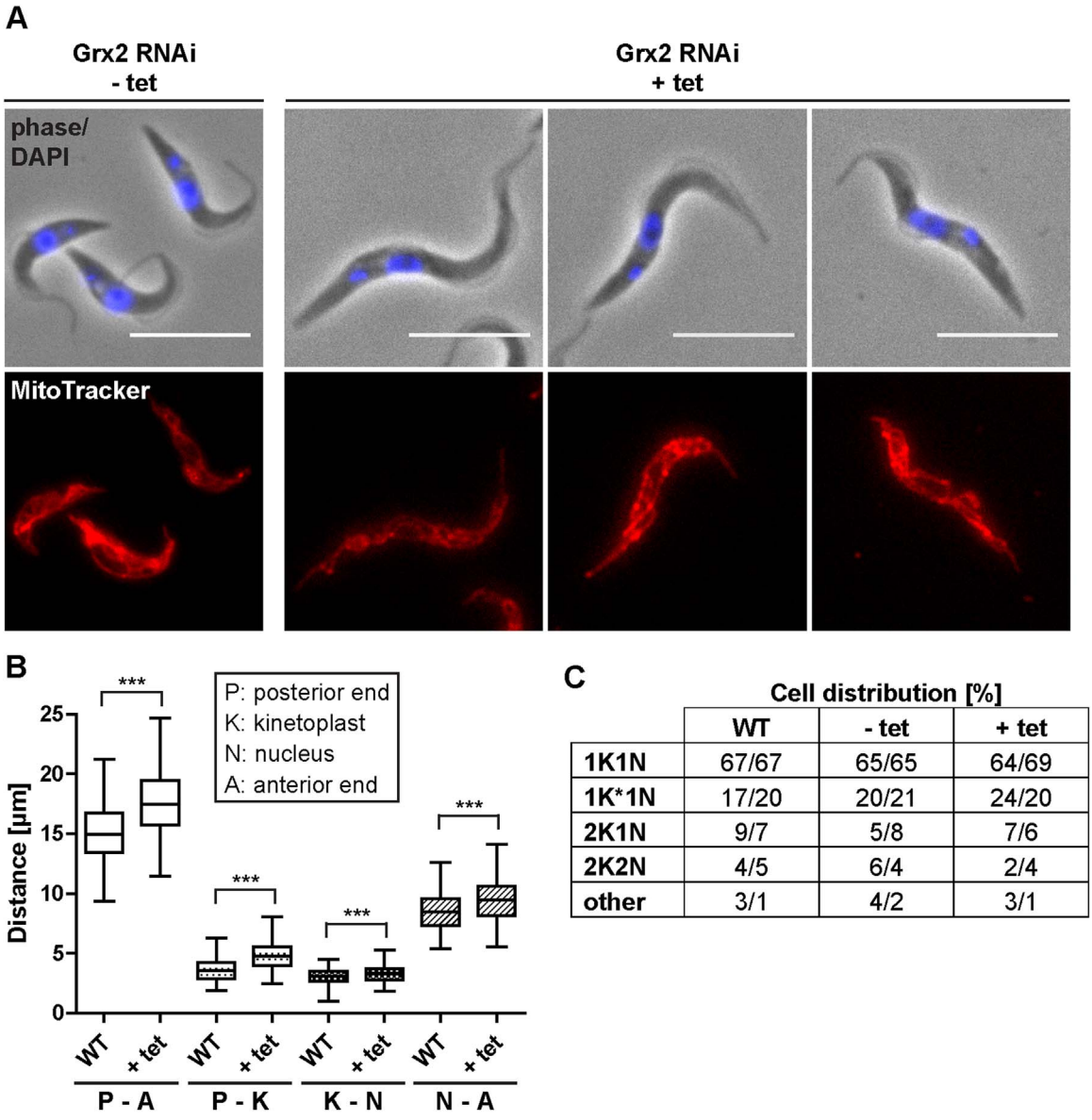

	WT	- tet	+ tet
1K1N	67/67	65/65	64/69
1K*1N	17/20	20/21	24/20
2K1N	9/7	5/8	7/6
2K2N	4/5	6/4	2/4
other	3/1	4/2	3/1

Fig. 11. Morphological analysis of Grx2-depleted PC *T. brucei*. A. Grx2 RNAi cells grown for three days in the absence (- tet) and presence of tet (+ tet) were stained with MitoTracker and DAPI and analyzed by fluorescence microscopy. Induction of RNAi leads to an elongated phenotype. The merge of phase contrast and DAPI images (upper panel) as well as the MitoTracker staining (lower panel) are shown for representative cells. Scale bar: 10 µm. B. Quantification of cellular distances in 210 WT parasites and 210 Grx2-RNAi cells induced for 3 days (+ tet) with 1K1N configuration, irrespective of the overall cell morphology. The minimum, mean, and maximum distances as well as the mean distance ± standard deviations are depicted. Distances were measured using ImageJ software. The p-values were calculated by Student's unpaired *t*-test (***, p-value ≤ .001). C. Karyotype analysis of WT, non-induced (- tet) and induced (+ tet) Grx2 RNAi cells. At least 280 cells were inspected for their kinetoplast and nucleus content. The percentage of cells with the respective configuration is given for two independent experiments. 1K*1N are cells with one elongated kinetoplast and one nucleus. Other indicates cells with abnormal N-K distribution.

this task is taken over by the highly abundant Tpx. Tpx-depletion renders BS *T. brucei* extremely sensitive to a challenge with exogenous hydrogen peroxide [13]. Further evidence that maintenance of the overall cellular thiol redox homeostasis in the infective stage of the parasite does not depend on the dithiol Grxs was provided by heat-stress experiments. As shown here for the first time, a 2 °C increase (from 37 to 39 °C) of the culture temperature entails a marked shift of the intracellular thiol status to more oxidizing conditions. However, WT and Grx1/Grx2 KO cells displayed an identical increase of the TS_2/$T(SH)_2$ ratio and the level of S-glutathionylated proteins. A respective finding has been reported for *S. cerevisiae* where deletion of the genes for Grx1 and Grx2 does not affect the cellular glutathione redox state [39].

Instead, our data support a regulatory function of the dithiol Grxs in the adaptation of BS cells to elevated temperatures. WT parasites grown at 39 °C displayed a strongly attenuated proliferation in accordance with published data [28,29,49]. The distribution of cells in the different phases of the cell cycle changed dramatically. The strong decrease of cells with 1K1N configuration and increase in cells with 2K2N is consistent with a preferential arrest in a pre-cytokinesis state [60]. Compared to the WT parasites, the Grx2 KO culture retained a significantly higher growth rate at 39 °C together with a larger portion of cells with normal morphology and karyotype distribution. The heat-induced growth impairment of WT cells does not imply a putative altered subcellular distribution of Grx2 because the protein retained its mitochondrial localization in BS cells grown at either 37 °C or 39 °C. Remarkably, the same phenotype observed for Grx2 KO cells was found for Grx1/Grx2 KO cells and, as reported previously, for cells that specifically lack Grx1 [49]. This strongly suggests that the cytosolic Grx1 and the IMS-localized Grx2 work in series within a process that attenuates the proliferation of BS parasites at the elevated temperature.

Interestingly, the severe temperature sensitivity of WT BS cells was

restored when Grx2 KO cells ectopically expressed a copy of the authentic protein but neither the C31S/C34S nor C34S mutant indicating that the biological function of Grx2 is redox-dependent. Recombinant C34S Grx2 retained about 40% of the HEDS activity of the WT protein. Either the lowered deglutathionylation capacity of C34S Grx2 may not be sufficient to restore the WT phenotype or the Grx2 reaction in BS cells follows a dithiol mechanism. Dithiol Grxs catalyze both protein disulfide formation and S-glutathionylation as well as protein deglutathionylation and reduction of protein disulfides by GSH [9,19,4,55,64]. Notably, the import and productive folding of IMS proteins have been shown to be strongly affected by the thiol redox state and the presence or absence of dithiol Grxs. For instance, low concentrations of GSH stimulate the import and oxidative folding of IMS proteins whereas high GSH concentrations strongly diminish the translocation of IMS, but not of matrix proteins into isolated mitochondria [48,7]. Also, import and oxidative folding of IMS proteins are delayed in yeast cells that either lack dithiol Grxs or overexpress Grx2 in the IMS [31].

In fact, no disulfide isomerase has been identified in the IMS [7] and it has been speculated that IMS-localized Grxs might partake in proofreading thiol/disulfide reactions [31]. In trypanosomes oxidative protein folding in the IMS has not been studied in detail but the process appears to significantly differ from the canonical one in other organisms [23]. In virtually all eukaryotes, the oxidoreductase Mia40 and the sulfhydryl oxidase Erv1 form a redox relay that mediates the translocation of cysteine-rich proteins from the cytosol into the IMS [25]. Trypanosomes possess an essential Erv1 protein but lack Mia40 [3]. Taken together, the following hypothetical mechanism could be envisaged for dithiol Grxs in BS parasites: Under standard culture conditions, the cellular thiol redox milieu is strongly reducing and the Grxs are dispensable. Under the more oxidizing conditions generated by a rise in temperature, Grx1 and Grx2 could play a role in the import and productive folding of target proteins that reside permanently or transiently in the IMS and act as negative regulators of cell proliferation. In the absence of one or both Grxs, this regulatory step would be hampered or missing with the consequence that proliferation of the parasites is less affected. This could explain why BS cells that lack either Grx1 or Grx2 or both proteins displayed an identical phenotype. In this respect it is highly interesting that in smooth muscle cells, Grx1-depletion attenuates the cell growth defect upon heat stress [18]. Although the proteins involved are not the same, both studies link Grx-deficiency with increased cell proliferation at high temperature.

Infection of mice with Grx2 KO as well as Grx1/2 KO parasites resulted in high parasitemia like WT parasites showing that the oxidoreductases are not essential for the *in vivo* infectivity. However, the mouse model may not be ideal for studies on a putative fever effect the parasites may encounter in their mammalian hosts. As reported recently, mice respond to an infection with African trypanosomes even with a hypothermia of their surface body temperature [8].

In the insect stage, Grx2 is essential. Here we show that PC cells require a distinct level of redox active Grx2 for viability. Parasites in which one *grx2* allele was deleted displayed a transient reduction of the Grx2 protein level which was accompanied by an attenuated proliferation. Upon prolonged cultivation, both effects got lost indicating that the cells managed to restore WT level of Grx2. The second allele could be replaced if the cells harbored an ectopic copy of WT or C34S Grx2, but not the C31S/C34S mutant. This strongly suggests that the IMS-localized oxidoreductase has an essential redox function in this life cycle stage. Conditional Grx2 KO cells that expressed the C34S mutant proliferated at about 75% of the rate of WT cells. Thus, the authentic protein may be slightly more efficient, but clearly, the physiological function of Grx2 does not require a dithiol mechanism. This fits to the fact that all putative *Leishmania* orthologues lack the second active site cysteine and thus can undergo exclusively monothiol reactions.

Depletion of the mRNA of Grx2 in PC cells causes a proliferation defect [9]. As shown here, after several days of RNAi induction the growth arrest got lost which was associated with re-appearance of the protein, a phenomenon often observed for essential proteins in trypanosomes [62]. When cultured at 37 °C, the relative proliferation defect due to Grx2-depletion was identical to that in cells grown at 27 °C. Evidently, Grx2 does not play a role in the heat-stress response of PC parasites.

The Grx2-depleted cells ceased proliferation but dead cells were not detectable. Remarkably, many cells displayed an elongated cell body. This morphological restructuring involved modulation of the posterior end to kinetoplast as well as kinetoplast to nucleus and nucleus to anterior end dimension. Therefore it differed from the specific extended posterior end morphology found in PC cells that ectopically express the Zink finger protein ZFP2 [24] or are depleted of cyclin 2 or sphingosine kinase [22,53]. In common with cyclin 2- or sphingosin kinase-depleted PC cells [22,53], the proliferation of the Grx2-depleted cells remained attenuated when the cells were re-transferred into tet-free medium suggesting that the absence of Grx2 induced an irreversible alteration. Elongation of the cell body in the Grx2-depleted cells was accompanied by a corresponding extension of the single mitochondrion. A similar phenomenon has been reported for PC *T. brucei* upon depletion of the cdc2-related kinases 1 and 2. In these cells, the posterior end is extended and/or branched and the mitochondrion expands into these extended spaces [63].

When grown in the presence of high glucose, the Grx2-depleted PC cells retained a slightly higher proliferation rate when compared to standard low-glucose conditions. A significant effect on the NADPH level is unlikely since PC *T. brucei* have two NADPH-producing pathways that are redundant under both high- and low-glucose conditions [2]. In high-glucose medium, PC parasites no longer require ATP synthase but obtain ATP by substrate level phosphorylation [15]. Grx2 might play a role in protecting or regulating a component of the respiratory chain and thus the energy metabolism of the cell. Regulation of respiratory chain complexes is a well-known function of Grx2 in the mitochondrial matrix of mammalian cells [41,4,65]. In trypanosomes, small thioredoxin-type oxidoreductase appear to be absent from the mitochondrial matrix as so far neither Tpx nor a thioredoxin or Grx has been described in this compartment. Thus, a Grx2-catalyzed redox regulation or protection of a respiratory chain component from the IMS site may occur. However, such a role of Grx2 becomes less relevant when oxidative phosphorylation is diminished.

5. Conclusions

The function of Grx2 in *T. brucei* is dependent of the life cycle stage. In BS cells, Grx2 is not essential neither *in vitro* nor *in vivo*. However, the oxidoreductase contributes to the reversible growth arrest BS parasites encounter under conditions that mimic a fever situation in the mammalian host. In PC cells, Grx2 is essential. Depletion of the oxidoreductase strongly affects the cell morphology and causes an irreversible proliferation arrest. Using trypanosomes as model organism, we show that a redox active dithiol Grx in the mitochondrial IMS can have cell type-specific regulatory roles for the proliferation and morphology of the cell.

Acknowledgments

The work of R.L.K.-S. was supported by the Deutsche Forschungsgemeinschaft (Priority Programme on „Dynamics of thiol-based redox switches in cellular physiology“, DFG Kr 1242/6-1 and Kr 1242/8-1). M.A.C. acknowledges the support of ICGEB grant CRP/URU14-01 and the technical assistance of Gabriel Fernández (Transgenic and Experimental Animal Unit, Institut Pasteur de Montevideo).

Conflict of interest

The authors declare that there are no conflicts of interest.

Appendix A. Supplementary material

Supplementary data associated with this article can be found in the online version at http://dx.doi.org/10.1016/j.redox.2018.01.011.

References

[1] E.M. Allen, J.J. Mieyal, Protein-thiol oxidation and cell death: regulatory role of glutaredoxins, Antioxid. Redox Signal 17 (2012) 1748–1763.
[2] S. Allmann, P. Morand, C. Ebikeme, L. Gales, M. Biran, J. Hubert, A. Brennand, M. Mazet, J.M. Franconi, P.A. Michels, et al., Cytosolic NADPH homeostasis in glucose-starved procyclic Trypanosoma brucei relies on malic enzyme and the pentose phosphate pathway fed by gluconeogenic flux, J. Biol. Chem. 288 (2013) 18494–18505.
[3] S. Basu, J.C. Leonard, N. Desai, D.A. Mavridou, K.H. Tang, A.D. Goddard, M.L. Ginger, J. Lukes, J.W. Allen, Divergence of Erv1-associated mitochondrial import and export pathways in trypanosomes and anaerobic protists, Eukaryot. Cell 12 (2013) 343–355.
[4] S.M. Beer, E.R. Taylor, S.E. Brown, C.C. Dahm, N.J. Costa, M.J. Runswick, M.P. Murphy, Glutaredoxin 2 catalyzes the reversible oxidation and glutathionylation of mitochondrial membrane thiol proteins: implications for mitochondrial redox regulation and antioxidant defense, J. Biol. Chem. 279 (2004) 47939–47951.
[5] P. Begas, L. Liedgens, A. Moseler, A.J. Meyer, M. Deponte, Glutaredoxin catalysis requires two distinct glutathione interaction sites, Nat. Commun. 8 (2017) 14835.
[6] S. Biebinger, L.E. Wirtz, P. Lorenz, C. Clayton, Vectors for inducible expression of toxic gene products in bloodstream and procyclic Trypanosoma brucei, Mol. Biochem. Parasitol. 85 (1997) 99–112.
[7] M. Bien, S. Longen, N. Wagener, I. Chwalla, J.M. Herrmann, J. Riemer, Mitochondrial disulfide bond formation is driven by intersubunit electron transfer in Erv1 and proofread by glutathione, Mol. Cell 37 (2010) 516–528.
[8] G. Caljon, N. Van Reet, C. De Trez, M. Vermeersch, D. Perez-Morga, J. Van Den Abbeele, The dermis as a delivery site of Trypanosoma brucei for Tsetse flies, PLoS Pathog. 12 (2016) e1005744.
[9] S. Ceylan, V. Seidel, N. Ziebart, C. Berndt, N. Dirdjaja, R.L. Krauth-Siegel, The dithiol glutaredoxins of african trypanosomes have distinct roles and are closely linked to the unique trypanothione metabolism, J. Biol. Chem. 285 (2010) 35224–35237.
[10] W.H. Chung, K.D. Kim, Y.J. Cho, J.H. Roe, Differential expression and role of two dithiol glutaredoxins Grx1 and Grx2 in Schizosaccharomyces pombe, Biochem. Biophys. Res. Commun. 321 (2004) 922–929.
[11] M. Comini, U. Menge, L. Flohe, Biosynthesis of trypanothione in Trypanosoma brucei brucei, Biol. Chem. 384 (2003) 653–656.
[12] M.A. Comini, R.L. Krauth-Siegel, M. Bellanda, Mono- and dithiol glutaredoxins in the trypanothione-based redox metabolism of pathogenic trypanosomes, Antioxid. Redox Signal 19 (2013) 708–722.
[13] M.A. Comini, R.L. Krauth-Siegel, L. Flohe, Depletion of the thioredoxin homologue tryparedoxin impairs antioxidative defence in African trypanosomes, Biochem J. 402 (2007) 43–49.
[14] V. Coustou, S. Besteiro, L. Riviere, M. Biran, N. Biteau, J.M. Franconi, M. Boshart, T. Baltz, F. Bringaud, A mitochondrial NADH-dependent fumarate reductase involved in the production of succinate excreted by procyclic Trypanosoma brucei, J. Biol. Chem. 280 (2005) 16559–16570.
[15] V. Coustou, M. Biran, M. Breton, F. Guegan, L. Riviere, N. Plazolles, D. Nolan, M.P. Barrett, J.M. Franconi, F. Bringaud, Glucose-induced remodeling of intermediary and energy metabolism in procyclic Trypanosoma brucei, J. Biol. Chem. 283 (2008) 16342–16354.
[16] M.L. Cunningham, M.J. Zvelebil, A.H. Fairlamb, Mechanism of inhibition of trypanothione reductase and glutathione reductase by trivalent organic arsenicals, Eur. J. Biochem 221 (1994) 285–295.
[17] M.P. Cunningham, K. Vickerman, Antigenic analysis in the Trypanosoma brucei group, using the agglutination reaction, Trans. R. Soc. Trop. Med. Hyg. 56 (1962) 48–59.
[18] D. Das, Y.H. Wang, C.Y. Hsieh, Y.J. Suzuki, Major vault protein regulates cell growth/survival signaling through oxidative modifications, Cell. Signal. 28 (2016) 12–18.
[19] Y. Du, H. Zhang, X. Zhang, J. Lu, A. Holmgren, Thioredoxin 1 is inactivated due to oxidation induced by peroxiredoxin under oxidative stress and reactivated by the glutaredoxin system, J. Biol. Chem. 288 (2013) 32241–32247.
[20] A.H. Fairlamb, G.B. Henderson, A. Cerami, Trypanothione is the primary target for arsenical drugs against African trypanosomes, Proc. Natl. Acad. Sci. USA 86 (1989) 2607–2611.
[21] A.P. Fernandes, A. Holmgren, Glutaredoxins: glutathione-dependent redox enzymes with functions far beyond a simple thioredoxin backup system, Antioxid. Redox Signal 6 (2004) 63–74.
[22] T.C. Hammarton, M. Engstler, J.C. Mottram, The Trypanosoma brucei cyclin, CYC2, is required for cell cycle progression through G1 phase and for maintenance of procyclic form cell morphology, J. Biol. Chem. 279 (2004) 24757–24764.
[23] A. Harsman, A. Schneider, Mitochondrial protein import in trypanosomes: expect the unexpected, Traffic 18 (2017) 96–109.
[24] E.F. Hendriks, D.R. Robinson, M. Hinkins, K.R. Matthews, A novel CCCH protein which modulates differentiation of Trypanosoma brucei to its procyclic form, EMBO J. 20 (2001) 6700–6711.
[25] J.M. Herrmann, J. Riemer, Mitochondrial disulfide relay: redox-regulated protein import into the intermembrane space, J. Biol. Chem. 287 (2012) 4426–4433.
[26] C. Hiller, A. Nissen, D. Benitez, M.A. Comini, R.L. Krauth-Siegel, Cytosolic peroxidases protect the lysosome of bloodstream African trypanosomes from iron-mediated membrane damage, PLoS Pathog. 10 (2014) e1004075.
[27] A. Holmgren, Thioredoxin catalyzes the reduction of insulin disulfides by dithiothreitol and dihydrolipoamide, J. Biol. Chem. 254 (1979) 9627–9632.
[28] L. Izquierdo, A. Atrih, J.A. Rodrigues, D.C. Jones, M.A. Ferguson, Trypanosoma brucei UDP-glucose:glycoprotein glucosyltransferase has unusual substrate specificity and protects the parasite from stress, Eukaryot. Cell 8 (2009) 230–240.
[29] B.C. Jensen, C.T. Kifer, M. Parsons, Trypanosoma brucei: two mitogen activated protein kinase kinases are dispensable for growth and virulence of the bloodstream form, Exp. Parasitol. 128 (2011) 250–255.
[30] M. Keil, B. Bareth, M.W. Woellhaf, V. Peleh, M. Prestele, P. Rehling, J.M. Herrmann, Oxa1-ribosome complexes coordinate the assembly of cytochrome C oxidase in mitochondria, J. Biol. Chem. 287 (2012) 34484–34493.
[31] K. Kojer, V. Peleh, G. Calabrese, J.M. Herrmann, J. Riemer, Kinetic control by limiting glutaredoxin amounts enables thiol oxidation in the reducing mitochondrial intermembrane space, Mol. Biol. Cell 26 (2015) 195–204.
[32] N.S. Kosower, E.M. Kosower, Formation of disulfides with diamide, Methods Enzymol. 143 (1987) 264–270.
[33] R.L. Krauth-Siegel, M.A. Comini, Redox control in trypanosomatids, parasitic protozoa with trypanothione-based thiol metabolism, Biochim Biophys. Acta 1780 (2008) 1236–1248.
[34] R.L. Krauth-Siegel, A.E. Leroux, Low-molecular-mass antioxidants in parasites, Antioxid. Redox Signal 17 (2012) 583–607.
[35] N. Lamour, L. Riviere, V. Coustou, G.H. Coombs, M.P. Barrett, F. Bringaud, Proline metabolism in procyclic Trypanosoma brucei is down-regulated in the presence of glucose, J. Biol. Chem. 280 (2005) 11902–11910.
[36] C.H. Lillig, C. Berndt, A. Holmgren, Glutaredoxin systems, Biochim Biophys. Acta 1780 (2008) 1304–1317.
[37] C. Lind, R. Gerdes, Y. Hamnell, I. Schuppe-Koistinen, H.B. von Lowenhielm, A. Holmgren, I.A. Cotgreave, Identification of S-glutathionylated cellular proteins during oxidative stress and constitutive metabolism by affinity purification and proteomic analysis, Arch. Biochem. Biophys. 406 (2002) 229–240.
[38] B. Liu, J. Wang, N. Yaffe, M.E. Lindsay, Z. Zhao, A. Zick, J. Shlomai, P.T. Englund, Trypanosomes have six mitochondrial DNA helicases with one controlling kinetoplast maxicircle replication, Mol. Cell 35 (2009) 490–501.
[39] S. Luikenhuis, G. Perrone, I.W. Dawes, C.M. Grant, The yeast Saccharomyces cerevisiae contains two glutaredoxin genes that are required for protection against reactive oxygen species, Mol. Biol. Cell 9 (1998) 1081–1091.
[40] M. Luthman, A. Holmgren, Glutaredoxin from calf thymus, Purif. Homog. J. Biol. Chem. 257 (1982) 6686–6690.
[41] R.J. Mailloux, J.R. Treberg, Protein S-glutathionlyation links energy metabolism to redox signaling in mitochondria, Redox Biol. 8 (2016) 110–118.
[42] J.M. Mansfield, D.M. Paulnock, Regulation of innate and acquired immunity in African trypanosomiasis, Parasite Immunol. 27 (2005) 361–371.
[43] B. Manta, M. Bonilla, L. Fiestas, M. Sturlese, G. Salinas, M. Bellanda, M.A. Comini, Polyamine-based thiols in trypanosomatids: evolution, protein structural adaptations, and biological functions, Antioxid. Redox Signal. (2017).
[44] B. Manta, M. Comini, A. Medeiros, M. Hugo, M. Trujillo, R. Radi, Trypanothione: a unique bis-glutathionyl derivative in trypanosomatids, Biochim Biophys. Acta 1830 (2013) 3199–3216.
[45] B. Manta, C. Pavan, M. Sturlese, A. Medeiros, M. Crispo, C. Berndt, R.L. Krauth-Siegel, M. Bellanda, M.A. Comini, Iron-sulfur cluster binding by mitochondrial monothiol glutaredoxin-1 of Trypanosoma brucei: molecular basis of iron-sulfur cluster coordination and relevance for parasite infectivity, Antioxid. Redox Signal 19 (2013) 665–682.
[46] V.E. Marquez, D.G. Arias, M.L. Chiribao, P. Faral-Tello, C. Robello, A.A. Iglesias, S.A. Guerrero, Redox metabolism in Trypanosoma cruzi. Biochemical characterization of dithiol glutaredoxin dependent cellular pathways, Biochimie 106 (2014) 56–67.
[47] V.E. Marquez, D.G. Arias, C.V. Piattoni, C. Robello, A.A. Iglesias, S.A. Guerrero, Cloning, expression, and characterization of a dithiol glutaredoxin from Trypanosoma cruzi, Antioxid. Redox Signal 12 (2010) 787–792.
[48] N. Mesecke, N. Terziyska, C. Kozany, F. Baumann, W. Neupert, K. Hell, J.M. Herrmann, A disulfide relay system in the intermembrane space of mitochondria that mediates protein import, Cell 121 (2005) 1059–1069.
[49] B. Musunda, D. Benitez, N. Dirdjaja, M.A. Comini, R.L. Krauth-Siegel, Glutaredoxin-deficiency confers bloodstream Trypanosoma brucei with improved thermotolerance, Mol. Biochem. Parasitol. 204 (2015) 93–105.
[50] F.R. Opperdoes, P. Baudhuin, I. Coppens, C. De Roe, S.W. Edwards, P.J. Weijers, O. Misset, Purification, morphometric analysis, and characterization of the glycosomes (microbodies) of the protozoan hemoflagellate Trypanosoma brucei, J. Cell Biol. 98 (1984) 1178–1184.
[51] S.L. Oza, M.R. Ariyanayagam, N. Aitcheson, A.H. Fairlamb, Properties of trypanothione synthetase from Trypanosoma brucei, Mol. Biochem. Parasitol. 131 (2003) 25–33.
[52] H.V. Pai, D.W. Starke, E.J. Lesnefsky, C.L. Hoppel, J.J. Mieyal, What is the functional significance of the unique location of glutaredoxin 1 (GRx1) in the intermembrane space of mitochondria? Antioxid. Redox Signal 9 (2007) 2027–2033.
[53] D.A. Pasternack, A.I. Sharma, C.L. Olson, C.L. Epting, D.M. Engman, Sphingosine

kinase regulates microtubule dynamics and organelle positioning necessary for proper G1/S Cell Cycle Transition in Trypanosoma brucei, MBio 6 (2015) (e01291-01215).
[54] C.D. Peikert, J. Mani, M. Morgenstern, S. Kaser, B. Knapp, C. Wenger, A. Harsman, S. Oeljeklaus, A. Schneider, B. Warscheid, Charting organellar importomes by quantitative mass spectrometry, Nat. Commun. 8 (2017) 15272.
[55] A.V. Peskin, P.E. Pace, J.B. Behring, L.N. Paton, M. Soethoudt, M.M. Bachschmid, C.C. Winterbourn, Glutathionylation of the active site cysteines of peroxiredoxin 2 and recycling by glutaredoxin, J. Biol. Chem. 291 (2016) 3053–3062.
[56] L. Riviere, S.W. van Weelden, P. Glass, P. Vegh, V. Coustou, M. Biran, J.J. van Hellemond, F. Bringaud, A.G. Tielens, M. Boshart, Acetyl: succinate CoA-transferase in procyclic Trypanosoma brucei. gene identification and role in carbohydrate metabolism, J. Biol. Chem. 279 (2004) 45337–45346.
[57] D.R. Robinson, T. Sherwin, A. Ploubidou, E.H. Byard, K. Gull, Microtubule polarity and dynamics in the control of organelle positioning, segregation, and cytokinesis in the trypanosome cell cycle, J. Cell Biol. 128 (1995) 1163–1172.
[58] A. Roldan, M.A. Comini, M. Crispo, R.L. Krauth-Siegel, Lipoamide dehydrogenase is essential for both bloodstream and procyclic Trypanosoma brucei, Mol. Microbiol. 81 (2011) 623–639.
[59] S. Romao, H. Castro, C. Sousa, S. Carvalho, A.M. Tomas, The cytosolic tryparedoxin of Leishmania infantum is essential for parasite survival, Int J. Parasitol. 39 (2009) 703–711.
[60] K.G. Rothberg, D.L. Burdette, J. Pfannstiel, N. Jetton, R. Singh, L. Ruben, The RACK1 homologue from Trypanosoma brucei is required for the onset and progression of cytokinesis, J. Biol. Chem. 281 (2006) 9781–9790.
[61] C. Schaffroth, M. Bogacz, N. Dirdjaja, A. Nissen, R.L. Krauth-Siegel, The cytosolic or the mitochondrial glutathione peroxidase-type tryparedoxin peroxidase is sufficient to protect procyclic Trypanosoma brucei from iron-mediated mitochondrial damage and lysis, Mol. Microbiol. 99 (2016) 172–187.
[62] T. Schlecker, A. Schmidt, N. Dirdjaja, F. Voncken, C. Clayton, R.L. Krauth-Siegel, Substrate specificity, localization, and essential role of the glutathione peroxidase-type tryparedoxin peroxidases in Trypanosoma brucei, J. Biol. Chem. 280 (2005) 14385–14394.
[63] X. Tu, J. Mancuso, W.Z. Cande, C.C. Wang, Distinct cytoskeletal modulation and regulation of G1-S transition in the two life stages of Trypanosoma brucei, J. Cell Sci. 118 (2005) 4353–4364.
[64] K. Ulrich, C. Finkenzeller, S. Merker, F. Rojas, K. Matthews, T. Ruppert, R.L. Krauth-Siegel, Stress-induced protein S-Glutathionylation and S-Trypanothionylation in African Trypanosomes-A quantitative redox proteome and thiol analysis, Antioxid. Redox Signal 27 (2017) 517–533.
[65] F. Yin, H. Sancheti, E. Cadenas, Mitochondrial thiols in the regulation of cell death pathways, Antioxid. Redox Signal 17 (2012) 1714–1727.
[66] F. Zahedi Avval, A. Holmgren, Molecular mechanisms of thioredoxin and glutaredoxin as hydrogen donors for mammalian s phase ribonucleotide reductase, J. Biol. Chem. 284 (2009) 8233–8240.
[67] H. Zimmermann, I. Subota, C. Batram, S. Kramer, C.J. Janzen, N.G. Jones, M. Engstler, A quorum sensing-independent path to stumpy development in Trypanosoma brucei, PLoS Pathog. 13 (2017) e1006324.